NBSIR 88-3707

Prediction of Response Time of Smoke Detectors in Enclosure Fires

Yukio Yamauchi
Guest Scientist
Hochiki Corporation
Tokyo 194 Japan

U.S. DEPARTMENT OF COMMERCE
National Bureau of Standards
National Engineering Laboratory
Center for Fire Research
Gaithersburg, MD 20899

January 1988

Sponsored by
Hochiki Corporation
Tokyo 194 Japan

NBSIR 88-3707

PREDICTION OF RESPONSE TIME OF SMOKE DETECTORS IN ENCLOSURE FIRES

Yukio Yamauchi
Guest Scientist
Hochiki Corporation
Tokyo 194 Japan

U.S. DEPARTMENT OF COMMERCE
National Bureau of Standards
National Engineering Laboratory
Center for Fire Research
Gaithersburg, MD 20899

January 1988

Sponsored by
Hochiki Corporation
Tokyo 194 Japan

U.S. DEPARTMENT OF COMMERCE, C. William Verity, *Secretary*
NATIONAL BUREAU OF STANDARDS, Ernest Ambler, *Director*

TABLE OF CONTENTS

TABLE

LIST OF FIGURES

NBSIR 88-3707

Prediction of Response Time of Smoke Detectors in Enclosure Fires

Yukio Yamauchi

Guest Scientist
Center for Fire Research
National Bureau of Standards

ABSTRACT

In order to predict the response time of smoke detectors in enclosure fires, a computational model is developed for calculating the local particulate concentration near the ceiling. The large scale smoke movement is approximated by integral equations for the plume and ceiling-jet, which originates in the cold lower layer and penetrates into the accumulated smoke layer in the upper portion of enclosure. The effect of coagulation, which changes the particle size distribution, is included to enable predictions of an ionization smoke detector response. This engineering model is designed to be used in combination with two-layer zone models for obtaining more detailed information of smoke concentration in the upper layer. Sample calculations have been made and comparisons with relevant experimental data showed a reasonable agreement both in the mass concentration and particle number concentration of smoke in the ceiling-jet.

1. INTRODUCTION

Comprehensive fire models like those of Mitler and Emmons [1], and Jones [2] have paved the way for the deterministic assessment of potential fire hazards in buildings. One of the most important elements in performing a hazard analysis is the time of detection. Earlier detection of fire can provide a better safety margin to evacuat building occupants. Further, early detection is necessary for rapid notification of the fire department and for rapid initiation of automatic fire suppression. A great deal of research has already been done to understand the response of the heat sensitive devices, such as automatic sprinklers, but fewer studies have been made in relation to the response of smoke detectors.

Two types of smoke detectors are in common use today: the photo-electric type and the ionization type. These two types of detectors operate on fundamentally different physical principles. The photo-electric smoke detectors use the scattering of light by smoke particles. The ionization smoke detectors use the reduction of ion current in an ionization chamber caused by the attachment of

ions to smoke particles. Both theoretical and experimental studies [3,4] show that the response functions of these detectors are strongly dependent on the number concentration and the size of smoke particles. Thus, in order to develop a predictive method for the response of smoke detectors, one must include the effects influencing the particulate component of smoke characteristics in addition to a model for large scale smoke movement.

Smoke aerosol generated at a fire source is carried upward as part of a buoyant plume. The plume then impinges on the ceiling and forms a radial outward flow under the ceiling. The nature of the flow is generally turbulent with strong entrainment; this dilutes the smoke aerosol during its way to the detector. The heat and particulate release rates are the most important factors influencing the smoke concentration near the ceiling. Further, accumulation of the smoke layer in the upper portion of the enclosure may vary the effect of dilution thus affecting the detector's response time.

Another influential effect on the response of smoke detectors is the coagulation of aerosol. At high concentration, smoke particles frequently collide and stick together as a result of Brownian motion. Through this process the average particle size increases while the particle number concentration decreases.

The first attempt to model the smoke dynamics in an enclosure fire has been made by Baum et al. [5]. In their model, the large scale fluid motion is directly calculated from the field equations of motion. Smoke movement is simulated by tracking mathematical "blobs" of smoke, and the effect of coagulation is treated as an internal process within each blob. In a previous study, the author has developed a model in which local particle number concentration is directly calculated from the field equation of coagulation [6]. However, there are difficulties in applying these field equation models to our engineering problems of detection, due to their requirement for very large computing facilities.

Recently, Evans [7] developed an engineering model for the prediction of the response time of automatic sprinklers. Based on the commonly used point source approximation, known as the Morton-Taylor-Turner model [8], Evans obtained an analytical solution for the plume flow in the two-layer environment of enclosure fires. A noticeable achievement in Evans' study is that he showed the prediction of response time of ceiling-mounted detectors is possible within the framework of two-layer zone models and with sufficient accuracy.

Following Evans' study, prediction of response time of smoke detectors on the basis of a zone model is now possible. In this report, a method is presented for approximating the large scale smoke movement in plume and ceiling-jet, which originates in the cold lower layer and penetrates into the accumulated smoke layer in the upper portion of the enclosure. The effect of coagulation is included to enable predictions of the response of ionization smoke detectors. Results of comparison with relevant experimental data are also described.

2. PLUME REGION

2.1 Governing Equations

Similar to Evans' study, the Morton-Taylor-Turner model is used as a basis for the present plume model in a two-layer environment.

The major assumptions of the present model are:

(1) The fire plume is axisymmetric and steady with no swirl;
(2) The environment is stagnant and stratified;
(3) The density (temperature) and the particulate concentration in each layer are uniform;
(4) The vertical velocity, temperature and particulate concentration have Gaussian profiles in the radial direction;
(5) The ideal gas law is valid;
(6) The Boussinesq approximation is valid.

The profiles of velocity, temperature and particulate concentration can be written as follows:

$$u/u_m = \exp(-r^2/b^2), \tag{1}$$

$$\Delta T/\Delta T_m = \Delta C_s/\Delta C_{sm} = \exp[-r^2/(\lambda b)^2]. \tag{2}$$

where $\Delta T = T - T_a$ and $\Delta C_s = C_s - C_{sa}$ represent respectively the temperature difference and the concentration difference from ambient, and b(z) is the 1/e width of the plume with respect to the velocity distribution. The profiles of the temperature and the particulate concentration are assumed to be identical.

With the above assumptions, the governing equations for mass, momentum, energy and particulate concentration can be written as follows:

$$\frac{d}{dz}\left(\int_0^\infty r\,u\,dr\right) = b\,\alpha\,u_m, \tag{3}$$

$$\frac{d}{dz}\left(\int_0^\infty r\,u^2\,dr\right) = \int_0^\infty r\,g\,\frac{\Delta T}{T_a}\,dr, \tag{4}$$

$$\frac{d}{dz}\left(\int_0^\infty r\, u\, \rho_a\, C_p\, (T - T_r)\, dr\right) = b\, \alpha\, u_m\, \rho_a\, C_p\, (T_a - T_r), \tag{5}$$

$$\frac{d}{dz}\left(\int_0^\infty r\, u\, (C_s - C_{sa})\, dr\right) = b\, \alpha\, u_m\, C_{sa}, \tag{6}$$

where α is the entrainment constant determined experimentally. T_a and C_{sa} represent respectively the ambient temperature and the ambient concentration at each height, and T_r is the arbitrary reference temperature.

Integration of Eqs. (3)-(6) yields the following relations governing plume flow in a stratified ambient:

$$\frac{d}{dz}(b^2\, u_m) = 2\, b\, \alpha\, u_m, \tag{7}$$

$$\frac{d}{dz}(b^2\, u_m^2) = 2\, \lambda^2\, b^2\, g\, \frac{\Delta T_m}{T_a}, \tag{8}$$

$$\frac{d}{dz}(b^2\, u_m\, \rho_a\, C_p\, \Delta T_m) = -\,(1 + 1/\lambda^2)\, b^2\, u_m\, \rho_a\, C_p\, \frac{dT_a}{dz}, \tag{9}$$

$$\frac{d}{dz}(b^2\, u_m\, \Delta C_{sm}) = -\,(1 + 1/\lambda^2)\, b^2\, u_m\, \frac{dC_{sa}}{dz}. \tag{10}$$

Eqs. (7)-(9) are equivalent to the equations used by Evans [7], and Eq. (10) for smoke concentration has been added in the same form as the energy equation. The plume flow in the upper layer is calculated directly from the governing equations by imposing boundary conditions at the interface between the upper and lower layer based on plume flow in the lower layer. This is similar to one of the several methods explored previously by Evans [7]. In deriving boundary conditions at the interface, it is assumed that the flux of mass, momentum, excess enthalpy, and smoke are conserved across the interface. Since each layer may be considered as having uniform temperature and smoke

concentration away from the plume flow region, the right hand side of Eqs. (9) and (10) are non-zero only at the interface.

The plume flow in the upper layer has to be solved numerically. In the program listed in APPENDIX, the fourth-order Runge-Kutta method is employed in obtaining a solution for the plume flow in the upper layer.

2.2 Parameters

The values of the entrainment constant α and Gaussian width ratio λ are necessary for evaluation of the plume model. From extensive experimental study, McCaffrey [9] provided a set of correlations for the centerline variations of temperature and velocity in buoyant diffusion flames. McCaffrey's correlations for the plume region ($0.20 < z/Q^{2/5}$) are consistent with the analytical solution of Eqs. (7)-(9) for homogeneous environment. Also, his data are believed to be the most reliable results available. Therefore, the values of α and λ were selected to match the McCaffrey's correlations.

Comparison of McCaffrey's correlations for the plume region with the analytical solution of Eqs. (7)-(9) yields the following values of α and λ:

$$\alpha = 0.118,$$

$$\lambda^2 = 1.157. \qquad (11)$$

These values will be used in all calculations to appear in this paper. They are slightly different but very close to the values used by Zukoski [10]: $\alpha = 0.110$, $\lambda^2 = 1.12$. It should be noted that the vertical coordinate z shall be taken as measured from the flame base to be consistent with McCaffrey's correlations.

2.3 Comparison with Experimental Data

Currently, no detailed smoke concentration data for the fire induced plumes are available. However, it is meaningful to evaluate this model using temperature data, since the smoke aerosols are believed to follow the same mechanism of transportation as temperature under adiabatic conditions.

Evans [7] provided one set of experimental data for plume centerline temperatures in a two-layer environment. Fig. 1 is a comparison of Evans' data with prediction. Although there is a sharp decrease in calculated plume temperature at the interface as pointed out by Evans, the overall agreement is quite good. This discontinuity of temperature can be smoothed out by simply assuming that the plume carries its lower-layer features to some distance into the upper layer (as shown by the dotted line in Fig. 1).

3. CEILING-JET REGION

3.1 Governing Equations

Incorporating the Boussinesq treatment for buoyancy and the Reynolds' analogy for convective heat transfer, Alpert [11] developed an integral model for the ceiling-jet induced by a fire under an unconfined ceiling. Alpert's theoretical predictions are in good agreement with the empirical correlations obtained by Alpert himself [12], and Pickard [13].

Assuming that the fire induced ceiling-jet confined in an enclosure behave the same way as an unconfined ceiling-jet with the environment of the upper layer, Alpert's model may be applied for calculating the near-ceiling smoke concentration as a function of radial distance from the fire axis.

The major assumptions are:

(1) The ceiling-jet is axisymmetric and steady with no swirl;
(2) The environment is stagnant and uniform;
(3) The velocity, temperature and particulate concentration have half-Gaussian profiles in the vertical direction;
(4) The ideal gas law is valid;
(5) The Boussinesq approximation is valid.

A detailed analysis of this type of flow can be found in Ref. [11]. Thus, only the final forms of the governing equations and a brief description will be presented here.

The vertical distribution functions of ceiling-jet velocity, temperature and smoke concentration can be obtained from Eq. (1) and (2) by replacing the coordinate r by y, and the length-scale b by ℓ; ℓ is the 1/e thickness of the ceiling-jet; implications for this is that the profiles are assumed to bear the same relationship as in the plume. The following are the integrated form of the governing equations for mass, momentum, energy and particulate concentration, respectively, for an axisymmetric ceiling-jet:

$$\frac{1}{r}\frac{d}{dr}(r\,\bar{v}\,h) = E\,\bar{v}, \tag{12}$$

$$\frac{1}{r}\frac{d}{dr}(r\,\bar{v}^2\,h) = -\frac{1}{2}f_w\,\bar{v}^2 - \frac{1}{2}\frac{d}{dr}\left[S\,g\,h^2\,\frac{\overline{\Delta T}}{T_a}\right], \tag{13}$$

$$\frac{1}{r}\frac{d}{dr}\left[r\,\bar{v}\,h\,\frac{\overline{\Delta T}}{T_a}\right] = -Q'', \tag{14}$$

$$\frac{1}{r}\frac{d}{dr}\left(r\,\bar{v}\,h\,\overline{\Delta C_s}\right) = 0, \tag{15}$$

where

$$f_w = \frac{\tau_w}{\rho_a\,\bar{v}^2\,/\,2}, \tag{16}$$

$$Q'' = \frac{h_w}{\rho_a\,C_p\,T_a}\left(\bar{T} - T_w\right). \tag{17}$$

The quantities $\bar{v}$, $\overline{\Delta T}$ and $\overline{\Delta C_s}$ appearing in Eqs. (12)-(15) are the spatially averaged values of the corresponding quantities in the ceiling-jet. The relations between the averaged and the maximum values are as follows:

$$\frac{\bar{v}}{v_m} = \frac{1}{\sqrt{2}},$$

$$\frac{\overline{\Delta T}}{\Delta T_m} = \frac{\overline{\Delta C_s}}{\Delta C_{sm}} = \sqrt{\frac{\lambda^2}{1+\lambda^2}},$$

$$\frac{h}{\ell} = \sqrt{\frac{\pi}{2}}. \tag{18}$$

The quantity S is the shape parameter which depends on the velocity and the temperature profiles. In the present case, S takes the value:

$$S = \frac{2\,\lambda^2}{\pi\,\sqrt{\lambda^2/(1+\lambda^2)}} \simeq 1.0. \tag{19}$$

By use of the Richardson number

$$R_i = \frac{g\ h\ \overline{\Delta T}}{\bar{v}^2\ T_a}, \tag{20}$$

the conservation equations of mass, momentum and energy can be combined into two separate equations for ceiling-jet thickness h and Richardson number R_i, which results as follows:

$$(1 - S\ R_i)\ \frac{dh}{dr} = \frac{1}{2}\ f_w + (2 - \frac{1}{2}\ S\ R_i)\ E - \frac{h}{r} - \frac{1}{2}\ S\ R_i\ \frac{Q''}{\bar{v}\ a}, \tag{21}$$

$$(1 - S\ R_i)\ \frac{h}{3R_i}\ \frac{dR_i}{dr} = \frac{1}{2}\ f_w + \left[1 + \frac{1}{2}\ S\ R_i\right]\left[E - \frac{Q''}{3\ \bar{v}\ a}\right] - (1 + 2\ S\ R_i)\ \frac{h}{3\ r}. \tag{22}$$

where $a = \overline{\Delta T}/T_a$.

The entrainment function E can be expressed as a function of the Richardson number R_i as:

$$E = E_o\ \exp[\beta\ (R_{io} - R_i)] \tag{23}$$

where β is an empirical constant; E_o and R_{io}, respectively, are the values of E and R_i at the start of the ceiling-jet.

The convective heat loss term $Q''/(\bar{v}a)$ can be correlated to the friction factor f_w by use of the Reynolds' analogy between the skin friction and the convective heat transfer:

$$S_t = \frac{h_w}{\rho_a\ C_p\ \bar{v}} = \frac{f_w}{2}\ \frac{1}{Pr^{2/3}}, \tag{24}$$

$$\frac{Q''}{\bar{v}\ a} = S_t\left(\frac{\bar{T} - T_w}{\bar{T} - T_a}\right) = K_w\ S_t. \tag{25}$$

$K_w = (T - T_w)/(T - T_a)$ characterizes the thermal conditions of the ceiling. $K_w = 0$ can be used for the adiabatic ceiling, and $K_w = 1$ can be used for the isothermal ceiling at $T_w = T_a$. The value of K_w may be calculated using the results of other fire models on wall and upper-layer temperatures.

Now, making use of Eqs. (23)-(25), and with proper boundary conditions, Eqs. (21) and (22) can be solved numerically. The other quantities of interest can be calculated by the following relationship:

$$\frac{\bar{v}}{\bar{v}_o} = \left(\frac{r\, R_i}{r_o\, R_{io}} \right)^{-1/3} \exp\left(- \frac{1}{3} \int_{ro}^{r} \frac{Kw\, S_t}{h}\, dr \right), \tag{26}$$

$$\frac{\overline{\Delta T}}{\overline{\Delta T}_o} = \frac{h_o}{h} \left(\frac{r_o^2\, R_i}{r^2\, R_{io}} \right)^{1/3} \exp\left(- \frac{2}{3} \int_{ro}^{r} \frac{K_w\, S_t}{h}\, dr \right), \tag{27}$$

$$\frac{\overline{\Delta C_s}}{\overline{\Delta C_{so}}} = \frac{h_o}{h} \left(\frac{r_o^2\, R_i}{r^2\, R_{io}} \right)^{1/3} \exp\left(\frac{1}{3} \int_{ro}^{r} \frac{K_w\, S_t}{h}\, dr \right), \tag{28}$$

where the subscript o denotes that they are the values at the exit of the stagnation region, i.e. up-stream boundary conditions for the ceiling-jet.

3.2 Parameters

The parameters necessary for calculations in ceiling-jets are the friction factor f_w, and E_o and β used in the entrainment function. In order to obtain the local values of f_w, Alpert calculated the thickness of the viscous sublayer formed between the ceiling and the main portion of ceiling-jet. However, as pointed out by Alpert himself, the value of f_w has little effect on the flow properties. In more recent experimental studies on fire induced ceiling-jets [14,15], values of f_w from 0.02 to 0.04 have been found to match the ceiling heat-transfer data. Further, You [16] pointed out that if the stagnation point heat flux is correlated, then $f_w = 0.025$ gives a best fit to their experimental data on ceiling heat transfer. In this study, f_w is assumed constant and the value 0.025 will be used.

Alpert assumed that the magnitude of entrainment at the start of the ceiling-jet is equal to the plume entrainment constant, and used $E_o = 0.12$ and $\beta = 3.9$. If the same assumption is applied to the present model, then E_o becomes 0.167 (0.118 for equivalent Gaussian profile). The value of E_o has a significant effect on the radial variation of smoke concentration and temperature, especially in the distance range of one or two ceiling-heights. Further, the initial entrainment need not necessarily be equal to the plume

entrainment constant. Therefore, several other values are tried in this study and their effect will be discussed.

3.3 Computation

Alpert provided the upstream boundary conditions for the ceiling-jet in relation to the impinging plume characteristics, which can be written with the present notations as follows:

$$h_o = b_p/\sqrt{6},$$

$$\bar{v}_o = u_{mp}/\sqrt{2},$$

$$\overline{\Delta T}_o = \frac{\lambda^2}{1 + \lambda^2} \Delta T_{mp},$$

$$\overline{\Delta C}_{so} = \frac{\lambda^2}{1 + \lambda^2} \Delta C_{smp}, \tag{29}$$

$$z_{jo} = H\ (1 + \sqrt{6}/5 \cdot \alpha)^{-1}. \tag{30}$$

The forth-order Runge-Kutta method is also used for numerical computations in the ceiling-jet.

3.4 Comparison with Experimental Data

In order to evaluate the ceiling-jet model, calculations for homogeneous environments are carried out and the results are compared with relevant experimental data on unconfined ceiling-jets.

Although minor differences exist due to variations in the plume related constants, almost identical results to Alpert's calculations are obtained for the ceiling-jet thickness, temperature and velocity, on the condition that the same values are used in E_o and β ($E_o = 0.12$, $\beta = 3.9$).

Veldman et al. [14] provided adiabatic ceiling-jet temperature data in their experimental study on ceiling heat transfer. Fig. 2 shows a comparison of their data with prediction. With $E_o = 0.12$, $\beta = 3.9$ and $K_w = 0$ (adiabatic condition), the calculation provides a correlation which fits the data quite nicely.

The data of Veldman et al. were obtained from laboratory scale experiments; heat release rates are between 1.17 kW and 1.53 kW and ceiling-heights are between 0.584 m and 0.813 m. On the other hand, Alpert's experimental correlations [12] were obtained from large scale tests with heat release rates ranging from 670 kW to 100 MW and ceiling heights from 4.6 m to 13.7 m. Since the present study is concerned with the very early stage of an enclosure fire, it is of great interest that prediction is compared with full scale experiments of small source strength (in the range of 100 kW).

Heskestad [17] provided experimental correlations obtained from fire tests with heat release rates in the range of 5 kW to 375 kW and the ceiling heights from 1.2 m to 2.4 m. Shown in Fig. 3 is a comparison between prediction of this model with Heskestad's correlation in radial variation of maximum excess temperatures. The agreement is again quite good. However, in obtaining this result, the initial magnitude of entrainment E_o was set to 0.05 which is about half of the value used by Alpert. Fig. 4 shows in the same way a comparison between the prediction and Heskestad's correlation in maximum velocities. The experimental and computational conditions are the same as in Fig. 3. Although general agreement can be seen, a consistent over-prediction is observed in this case.

The cause of inaccuracy in the velocity variations is not now understood, but it may be associated with the assumed Gaussian velocity profile. For the distance range greater than one ceiling height, the experimental correlation is very close to the calculated velocity values of equivalent top-hat profiles, which is $1/\sqrt{2}$ times less than the maximum velocities, suggesting decay of the Gaussian profile. This inaccuracy in velocity is not considered important in calculating the smoke detector's response time, since its dependence on the gas velocity is generally quite small. Thus, the values E_o = 0.05 and β = 3.9 will be used in the following calculations of ceiling-jets in room fire configurations.

4. FILLING PROCESS AND COAGULATION OF SMOKE

At high concentration, the particle number concentration of smoke changes quite rapidly by frequent particle collisions and sticking together. This effect of coagulation is specially important in quantifying the response of ionization smoke detectors, because their response functions are closely related to the number concentration of smoke aerosol. In the room configurations, this effect of coagulation may be estimated separately for the three regions of concern: plume, ceiling-jet and upper smoke-layer.

4.1 Coagulation in Plume and Ceiling-jet

Baum and Mulholland [18] presented a theory for the coagulation in a plume. According to their analysis, the problem of coagulation in the plume can be transformed into a problem of homogeneous coagulation by introducing the characteristic time τ_p defined by

$$\frac{d\tau_p}{dz} = \frac{\lambda^2 + 1}{2} [b(z)\ u_m(z)]^{-2}, \tag{31}$$

where $b(z)$ and $u_m(z)$, respectively are the Gaussian width and the maximum velocity in the plume as defined in Eqs. (1) and (2) of this paper. The particle number flux ϕ as a function of height can then be given by

$$\phi\ /\ \phi_o = 1\ /\ [1 + \Gamma\ \alpha_o\ \tau], \tag{32}$$

where Γ is the coagulation coefficient and ϕ_o is the initial number flux.

By applying the same analysis to the ceiling-jet, the following expression can be obtained for the characteristic time of ceiling-jet:

$$\frac{d\tau_j}{dr} = \sqrt{\frac{\lambda^2 + 1}{2}}\ [r\ \ell(r)\ v_m^2(r)]^{-1}. \tag{33}$$

Eq. (32) also applies for estimating the effect of coagulation in the ceiling-jet.

4.2 Filling Process and Coagulation

The problem of quantifying the effect of coagulation in the upper layer can be simplified by employing the commonly used assumption of two-layer zone models, i.e. the properties in the upper layer are uniform. The equations describing the conservation of mass and number concentration of smoke in the upper layer can generally be expressed as:

$$\frac{dM_s}{dt} = \dot{m}_{sp} - \dot{m}_{se}, \tag{34}$$

$$\frac{dN_s}{dt} = \dot{n}_{sp} - \dot{n}_{se} - \bar{K}_c,$$

$$\bar{K}_c = \int_0^V \Gamma \, n_s^2 \, dV, \tag{35}$$

where M_s and N_s, respectively, are the total mass and total particle number of smoke in the upper layer; $\dot{m}_{sp}$ and $\dot{n}_{sp}$ represent the source terms; $\dot{m}_{se}$ and $\dot{n}_{se}$ represent the loss of smoke through the doorway; n_s is the local number concentration of smoke; V is the volume of the upper layer.

With the assumption of homogeneous concentration, the coagulation term can be simplified as

$$\bar{K}_c = \int_0^V \Gamma \, \bar{n}_s^2 \, dV = \Gamma \, N_s^2 \, / \, V, \tag{36}$$

and the loss terms can be correlated to the total mass M, and the mass loss rate $\dot{m}_e$ of the gas in the upper layer:

$$\dot{m}_{se} = \left(\frac{\dot{m}_e}{M} \right) M_s,$$

$$\dot{n}_{se} = \left(\frac{\dot{m}_e}{M} \right) N_s. \tag{37}$$

Substitution of Eqs. (36)-(37) into Eqs. (34)-(35) yields:

$$\frac{dM_s}{dt} = \dot{m}_{sp} - \left(\frac{\dot{m}_e}{M}\right) M_s, \tag{38}$$

$$\frac{dN_s}{dt} = \dot{n}_{sp} - \frac{\rho\,\Gamma}{M} N_s^2 - \left(\frac{\dot{m}_e}{M}\right) N_s. \tag{39}$$

Expressing the equations in this form has the advantages that $\rho \cdot \Gamma$ is relatively insensitive to temperature and the model can be easily combined with other zone models by which values of M and $\dot{m}_e$ as functions of time may be provided. By further substituting $N' = N_s/M$ in equation 39, N′ becomes insensitive to expansion as the gas is heated.

Given the values of $\dot{M}$ and m_e, Eqs. (38) and (39) can be solved numerically. The mass and number concentration of smoke in the upper layer can then be obtained by dividing the variables by the upper-layer volume V:

$$C_s = M_s / V,$$

$$\bar{n}_s = N_s / V. \tag{40}$$

4.3 Simple model

We conduct a sample calculation here to make a rough estimate on the effect of coagulation in practical cases of early stage fire scenarios. As a typical case of ceiling height and detector location, we choose H = 3.0 m and r = 3.0 m, and the fire size, Q = 100 kW. Eq. (31) can be solved analytically for the case of uniform environment, which has the form:

$$\tau_p = 3 \left[\frac{9}{5} (\lambda^2 + 1)\, \alpha \right]^{-2/3} \left[\frac{g\,\dot{Q}}{\rho_a\, C_p\, T_a} \right]^{-2/3} (z_o^{-1/3} - z^{-1/3}). \tag{41}$$

Assuming that the flame height z_o is given by the relation $0.08 = z_o/Q^{2/5}$ (McCaffrey [9]), and z by Eqs. (30), a value $\tau_p = 3.3\ s^2/m^3$ can be obtained for $z_o = 0.5$ m, $z = 2.84$ m and $Q = 100$ kW. Numerical calculation of Eq. (33) gives $\tau_j = 2.1\ s^2/m^3$ at $r = 3.0$ m for the same source strength. The typical value of coagulation coefficient may be $\Gamma = 1.0 \times 10^{-15}\ m^3/s$ (Lee and Mulholland [19]). Now, substitution of the total characteristic time, $\tau = \tau_p + \tau_j$ into Eq. (32) gives the ratio of initial and local particle number flux ϕ / ϕ_o, as illustrated in Table 1.

Table 1 Effect of coagulation in plume and ceiling-jet: calculation.

ϕ_o	ϕ / ϕ_o		number concentration at r = 3.0 m
(particles/s)	r = 0.0 m($\tau = \tau_p$)	r = 3.0 m	(particles/m^3)
1.0×10^{12}	0.997	0.995	3.57×10^{11}
1.0×10^{13}	0.968	0.949	3.41×10^{12}
1.0×10^{14}	0.753	0.651	2.34×10^{13}
1.0×10^{15}	0.234	0.157	5.64×10^{13}
1.0×10^{16}	0.030	0.018	6.46×10^{13}

It can be seen from Table 1 that the total effect of coagulation in plume and ceiling-jet becomes quite important when the particle number flux exceeds the critical value of 10^{14} particles/sec. It also suggests that coagulation in the plume is more important than in the ceiling-jet, because its initial concentration is much higher than in the ceiling-jet. The effect of coagulation becomes even more important when the heat release rate has a smaller value. The critical number flux for a 10 kW source is approximately 10^{13} particles/sec.

The coagulation in the upper layer also plays a significant role in varying the smoke detectability, because it changes the environment of plume and ceiling-jet. If a time scale of 300 sec is assumed for the detector's response time, then the coagulation effect becomes important even for the number concentration of 10^{12} particles/m^3; the sensitivity of the ionization detector lies in this range.

It is believed that the number flux at the wall, where ceiling-jet ends, is fed into the upper layer. However, a quantitative model for describing this effect is not currently available. Therefore, more simplified model will be used here.

In the simple model, the effect of coagulation in plume and ceiling-jet is not directly calculated, but included in the source term of number concentration in the upper layer. If the coagulation in the ceiling-jet is neglected, then the effective particle number flux may be calculated by Eqs. (31) and (32), assuming the characteristic time τ does not change significantly by the presence of the accumulated upper smoke layer. By numerically integrating Eq. (39) using the effective number flux, the average number concentration in the upper layer can be obtained as a function of time. Now, using the effective number flux as a source term for the plume, the local number concentration in the ceiling-jet can be calculated by the same method described in Sec. 2 and 3 of this paper. Note that if the effect of coagulation is neglected, the equations for the number concentration become identical with the equations for the mass concentration of smoke. The exact form of equations for the number concentration can be obtained by replacing the variable C_s by n_s in Eqs. (6), (10), (15) and (28).

Based on the models described in Sec. 2, 3 and in this section, a subprogram has been developed for calculating the temperature, and mass and number concentration of smoke in ceiling-jet in a two-layer environment. The program needs input of the upper-layer thickness, average temperature and mass loss rate of gas through the doorway, which should be calculated by other two-layer zone models. The current version of the program is designed to be used in combination with the program FAST. FAST is a comprehensive multi-compartment fire model whose detailed description can be found in Ref. [2,20]. A complete list of the subprogram can be found in APPENDIX of this paper.

5. COMPARISON WITH EXPERIMENTS IN ROOM CONFIGURATIONS

Hochiki Corp. of Tokyo, Japan provided temperature and smoke concentration data collected in their test room for the purpose of evaluating the performance of smoke detectors. The size of the room is 6.0 m D. x 10.0 m W. x 4.0 m H. The effective ceiling-height can be changed to 3.0 m by placing additional floor-boards 1.0 m above the original floor. The walls are made of hollow concrete blocks of 25 cm thick, whose effective thickness may be about 5 cm. The ceiling is made of 1.6 cm thick gypsum plaster boards suspended from the concrete floor slab. The doorways and exhaust vents are sealed during the tests so that the only effective opening is a 30 cm x 30 cm drain hole located at the center of the floor. 17 thermocouples and 12 extinction meters are permanently installed in the test room to measure the radial and vertical distribution of temperature and smoke concentration. Additionally, one Measuring Ionization Chamber (MIC) [21] is mounted on the ceiling 3.0 m from the center. The MIC is a standard measuring device of smoke concentration used for testing the sensitivity of ionization smoke detectors. The MIC employs the same physical principle as ionization smoke detectors. The extinction meters used for the experiments have equivalent sensitivity to UL Standard specifications [22]. The extinction coefficient K can be obtained by the following relation from the meter readings:

$$K = \frac{1}{L} \ln \frac{I_o}{I}, \tag{42}$$

where L is the path length, I_o the intensity of incident light, and I the intensity of transmitted light.

The most generally used combustion materials for testing the performance of smoke detectors are: cotton, heptane, polyurethane and wood cribs. Among these, the heptane pool fire has been selected for making comparisons, since it can be regarded as a constant heat/smoke source with the exception of about 1 min of transient period after ignition.

The size of the pan used for the experiments is 33 cm x 33 cm and 5 cm deep, which was positioned on the floor at the center of the room. From mass loss data, the average heat release rate has been found to be approximately 85 kW. The extinction coefficient and MIC output taken at the point 3.0 m from the fire axis and 5 cm below the ceiling is used for comparison with prediction of ceiling-jet calculations.

Using the subprogram listed in APPENDIX in combination with the program FAST, calculations have been made for the two different ceiling heights, 3.0 and 4.0 m, for which experimental data were available. The heat release rate was assumed to rise exponentially in the first 1 min after ignition and then become constant (85 kW) after this transient period. The radiation loss fraction from the flame zone was assumed to be 0.30, which was subtracted from the heat release rate to obtain the effective heat flux of the plume. The mass generation rate of particulate $\dot{m}_p$ was assumed proportional to the mass flux of fuel, and the value of 0.0130 (Mulholland [23]) was used for the particle conversion ratio $\epsilon = \dot{m}_p/\dot{m}_f$, where $\dot{m}_f$ is the mass flux of fuel. The particle number flux was calculated by assuming a volume equivalent diameter $\bar{D}_v$ of 0.16 μm and the particulate density ρ_s of 2.0 x 10^3 kg/m^3:

$$\dot{n}_{sp} = \dot{m}_{sp} / (1/6 \cdot \pi \, \bar{D}_v^3 \, \rho_s). \tag{43}$$

The average particle size $\bar{D}_v$ has been determined by the experimental values of extinction coefficient and MIC output. The exact relation for obtaining the volume equivalent diameter will be shown in the latter part of this section.

There is a well accepted relation between the mass concentration of smoke and the extinction coefficient during flaming combustion:

$$K = \delta \, C_s, \tag{44}$$

where δ is a dimensional coefficient equal to 7.6×10^3 m^2/kg, which was found out experimentally by Seader and Einhorn [24], and Lee and Mulholland [19]. This relation is used to interpret the calculated mass concentration into the extinction coefficient.

The output of MIC is usually expressed by the quantity called Y-value, which was introduced by Hosemann [3] in his theoretical study on ionization chambers:

$$Y = \frac{i_o}{i} - \frac{i}{i_o}, \tag{45}$$

where i_o is the initial ionization current across the positive and negative electrodes and i is the ionization current in presence of smoke particles. According to his analysis, the Y-value is proportional to the product of the particle number concentration and effective particle diameter $n_s \cdot d$ as:

$$n_s \, \bar{d} = \eta \, Y, \tag{46}$$

where η is the chamber constant defined by

$$\eta = 3 \, \frac{\sqrt{\alpha_i \, q}}{C_B}. \tag{47}$$

In Eq. (47), q is the ion generation rate by the radio-active source, α_i is the recombination coefficient of ions and C_B is the Bricard attachment coefficient equal to 0.3 cm^2/sec. The value of $1/\eta$ characterizes the sensitivity of an ionization chamber. In an experimental analysis, Helsper et al. [25] showed that the value of $1/\eta$ for a Measuring Ionization Chamber is approximately 3.5×10^{-6} m^2. This value is used for making comparisons between the calculated number concentration and the MIC output.

Eqs. (44)-(47) have also been used to calculate the average particle size $\bar{D}_v$ of heptane smoke from the experimental values of extinction coefficient and MIC output. Given the instantaneous values of extinction coefficient and Y-value, the volume equivalent diameter $\bar{D}_v$ can be obtained by the following relation:

$$\bar{D}_v = \left[\frac{K}{Y} \frac{1}{\delta \eta (1/6 \cdot \pi \rho_s)} \right]^{1/2} . \qquad (48)$$

In obtaining the relation of Eq. (48), it has been assumed that the volume equivalent diameter D_v is equal to the effective average diameter d used in the response function of ionization smoke detectors. The only unknown parameter in Eq. (48) is the ratio of extinction coefficient to Y-value, K/Y. This parameter can be understood as a characteristic quantity influenced by the size and shape of smoke particles. The exact value of K/Y depends on the materials and the conditions of combustion.

In order to verify the calculations by FAST, the calculated upper-layer temperatures are compared with the temperature data taken at the points near the corners of the room and 5 cm below the ceiling. Fig. 5 and 6 show comparisons of calculated and measured upper-layer temperatures for two different ceiling heights. The experimental data shown are the average of temperatures taken at four different points; the distance of each point from the fire axis is identical (4.5 m) and its distance from the nearest wall is approximately 1.0 m. For both cases of ceiling height, the agreement between the prediction and measurement is quite good. From the fact that the temperatures have been measured near the ceiling, this may explain why the upper-layer temperatures are somewhat over-predicted. However, it may not pose an important effect on the calculations of smoke concentration.

Fig. 7 shows, in the same way, a comparison between the calculated and measured mass concentration of smoke in terms of extinction coefficient. The calculated result shown here is the output of FAST, thus representing the average mass concentration of smoke in the upper layer. The experimental data are for the point 5 cm below the ceiling and 3.0 m from the fire axis. Although an qualitative agreement can be seen between the two, there is a significant difference in a quantitative sense. This suggests that the smoke concentration in the ceiling-jet is much higher than the averaged values in the upper layer. Similar results have been obtained also in the case of 4.0 m ceiling height (Fig. 8).

Fig. 9 shows comparisons of ceiling-jet calculations with the experimental data for the mass concentration of smoke. The experimental data shown here are of the same location as in Fig. 5, and the calculated results are for the same radial position in the ceiling-jet. Although there are still small differences between the predictions and experimental data, the agreement is quite reasonable taking into account the fact that there is a 10 to 20 % uncertainty in the validity of Eq. (44) [19].

Finally, Fig. 10 shows a comparison of calculated and measured number concentration of smoke in the ceiling-jet in terms of MIC output. Similar to the results in Fig. 6, the calculation provides somewhat lower values than the experimental data. The general agreement is again quite reasonable. The decreasing rate of change of Y with respect to time is a result of a decreasing number concentration resulting from particle coagulation. It should be noted however that the assumption to set $\bar{D}_v$ and $\bar{d}$ equal may not be appropriate, since the exact relation between the two size parameters is not known for the smoke aerosol from flaming combustion, which usually has quite a complicated agglomerated shape. This leaves an uncertainty in the absolute value of calculated number concentration.

CONCLUSION

A method is described for calculating the local particulate concentration near the ceiling in an enclosure fire. The large scale smoke movement is approximated by integral equations for the plume and ceiling-jet, which originates in the cold layer and penetrates into the accumulated upper smoke layer. The effect of coagulation is treated by a simple two-layer zone model. The key source parameters are the fuel-to-particulate conversion ratio, the volume equivalent diameter of particulate and the heat release rate. Sample calculations have been made and comparisons with relevant experimental data showed a fairly encouraging result.

Direct measurement of number concentration in high density smoke, and a more detailed analysis on the response of smoke detectors especially for the particle of agglomerated shape, are desirable for validation and refinement of the model.

Presently, application of the model is limited to a fire source of flaming combustion. Refinements must be made before applying this model to smoldering combustion, which often precedes the flaming combustion in an early stage fire scenario.

ACKNOWLEDGEMENT

The author wishes to express his sincere thanks to the staff of the Center for Fire Research, National Bureau of Standards where this study has been performed. Special thanks are due to Richard Bukowski, George Mulholland, John Rockett, Walter Jones and Henri Mitler for their valuable suggestions and encouragement in the course of this study.

The author also wish to thank Hochiki Corp. of Tokyo, Japan for their support of this study and permission to use their experimental data.

NOMENCLATURE

a	$\overline{\Delta T}/T_a$
b	1/e width of plume [Eq. (1)]
C_B	Bricard attachment coefficient
C_p	specific heat
C_s	particulate-mass concentration
ΔC_s	particulate-concentration difference from ambient
d	effective average diameter of particulate [Eq. (46)]
D_v	volume equivalent diameter of particulate [Eq. (48)]
E	entrainment function of ceiling-jet
f_w	ceiling friction factor
g	gravitational acceleration
h	ceiling-jet thickness for equivalent top-hat profile
h_w	ceiling heat-transfer coefficient
I	light intensity
i	ionization current
K	extinction coefficient [Eq. (42)]
K_c	loss of particles by coagulation [Eq. (36)]
K_w	parameter of thermal boundary condition at ceiling [Eq. (25)]
L	path length of extinction meter
ℓ	1/e thickness of ceiling-jet
M	total mass of gas in upper layer
$\dot{m}$	mass flux of gas
M_s	total particulate-mass in upper layer
$\dot{m}_s$	particulate-mass flux
N_s	total number of particles in upper layer
n_s	particulate-number concentration
$\dot{n}_s$	particulate-number flux
P_r	Prandtl number
Q	heat release rate
Q''	parameter of ceiling heat transfer [Eq. (17)]
q	ion generation rate
R_i	Richardson number
r	radial distance from fire axis
S	shape parameter of ceiling-jet
S_t	Stanton number [Eq. (24)]
T	absolute temperature
ΔT	temperature difference from ambient
u	vertical velocity of plume
V	volume of upper layer
v	radial velocity of ceiling-jet
Y	Y-value of MIC output [Eq. (45)]
y	vertical distance measured from ceiling
z	vertical distance measured from plume source

Greek letters

α plume entrainment constant
α_i ion recombination coefficient
β parameter of entrainment [Eq. (23)]
Γ coagulation coefficient
δ constant defined by Eq. (44)
ϵ fuel-to-particulate conversion ratio
η chamber constant of ionization chamber
λ Gaussian width ratio [Eq. (2)]
ρ density
τ characteristic time of coagulation [Eq. (31), (33)]
τ_w ceiling shear stress
ϕ particle number flux

Superscripts

$\bar{}$ spatially averaged quantity

Subscripts

a ambient
e mass flux through doorway
f fuel
i interface
j ceiling-jet
l lower layer
m maximum value
o initial value
p plume
r reference state
s smoke particulate
u upper layer
w wall

REFERENCES

1. Mitler, H. and Emmons, H., Documentation for CFC V, The Fifth Harvard Computer Fire Code, Nat. Bur. of Stand. (U.S.), NBS-GCR 81-344, Oct. 1981.

2. Jones, W. W., A Model for the Transport of Fire, Smoke and Toxic Gases (FAST), Nat. Bur. of Stand. (U.S.), NBSIR 84-2934, Sept. 1984.

3. Hosemann, J. P., On the Theory of Ionization Chambers with Consideration of Small-Ion Recombination, Staub-Reinhalt. Luft, Vol. 32, No. 7, pp. 13-17, 1972.

4. Mulholland, G. W. and Liu, B. Y. H., Response of Smoke Detectors to Monodisperse Aerosols, J. Research Nat. Bur. Stand., Vol. 85, No. 3, pp.223-238, 1980.

5. Baum, H. R., Rehm, R. G. and Mulholland, G. W., Computation of Fire Induced Flow and Smoke Coagulation, 19th Symposium (International) on Combustion/The Combustion Inst., pp. 921-931, 1982.

6. Yamauchi, Y., Numerical Simulations of Smoke Movement and Coagulation, Proc. 1st International Symposium on Fire Safety Science, pp. 719-728, 1985.

7. Evans, D. D., Calculating Fire Plume Characteristics in a Two Layer Environment, Nat. Bur. Stand. (U.S.), NBSIR 83-2670, Sept. 1983.

8. Morton, B. R., Taylor, G. and Turner, J. S., Turbulent Gravitational Convection from Maintained and Instantaneous Sources, Proc. Roy. Soc., Lond. A., Vol. 234, pp. 1-23, 1956.

9. McCaffrey, B. J., Purely Buoyant Diffusion Flames: Some Experimental Results, Nat. Bur. Stand. (U.S.), NBSIR 79-1910, Oct. 1979.

10. Zukoski, E. E., Development of a Stratified Ceiling Layer in the Early Stages of a Closed-Room Fire, Fire and Materials, Vol. 2, No. 2, pp. 54-62, 1978.

11. Alpert, R. L., Turbulent Ceiling-Jet Induced by Large-Scale Fires, Combustion Science and Technology, Vol.11, pp.197-213, 1975.

12. Alpert, R. L., Calculation of Response Time of Ceiling-Mounted Fire Detectors, Fire Technology, Aug. 1972.

13. Pickard, R. W., Hird, D. and Nash, P., The Thermal Testing of Heat-Sensitive Fire Detectors, Fire Research Note No. 247, Fire Research Station, Borehamwood, Herts, England, 1957.

14. Veldman, C. C., Kubota, T. and Zukoski, E. E., An Experimental Investigation of the Heat Transfer from a Buoyant Gas Plume to a Horizontal Ceiling - Part 1. Unobstructed Ceiling, Nat. Bur. Stand. (U.S.), NBS-GCR 77-97, 1975.

15. You, H. Z. and Faeth, G. M., Ceiling Heat Transfer during Fire Plume and Fire Impingement, Fire and Materials, Vol.3, No. 3, pp. 140-147, 1979.

16. You, H. Z., An Investigation of Fire-Plume Impingement on a Horizonal Ceiling 2--Impingement and Ceiling-jet Regions, Fire and Materials, Vol. 9, No. 1, pp. 46-56, 1985.

17. Heskestad, G., Physical Modeling of Fire, J. Fire and Flammability, Vol. 6, pp. 253-273, 1975.

18. Baum, H. R. and Mulholland, G. W., Coagulation of Smoke Aerosol in a Buoyant Plume, J. Colloid and Interface Science, Vol. 72, No. 1, pp. 1-12, 1979.

19. Lee., T. G. K. and Mulholland, G. W., Physical Properties of Smokes Pertinent to Smoke Detector Technology, Nat. Bur. Stand. (U.S.), NBSIR 77-1312, Nov. 1977.

20. Walton, W. D., Baer, S. R. and Jones, W. W., User's Guide for FAST, Nat. Bur. Stand. (U.S.), NBSIR 85-3284, Dec. 1985.

21. Electronikcentralen, Horsholm Denmark, MIC Type EC 23095.

22. UL 268 Standard for Smoke Detectors for Fire Protective Signaling Systems, Underwrites Laboratories Inc.

23. Mulholland, G. W., private communication.

24. Seader, J. D. and Einhorn, I. N., Some Physical, Chemical, Toxicological, and Physiological Aspects of Fire Smokes, 16th Symposium (International) on Combustion/The Combustion Inst., pp. 1423-1445, 1976.

25. Helsper, C., Fissan, H., Muggli, J. and Sheidweiler, A., Verification of Ionization Chamber Theory, Fire Technology, pp. 14-21, Feb. 1983.

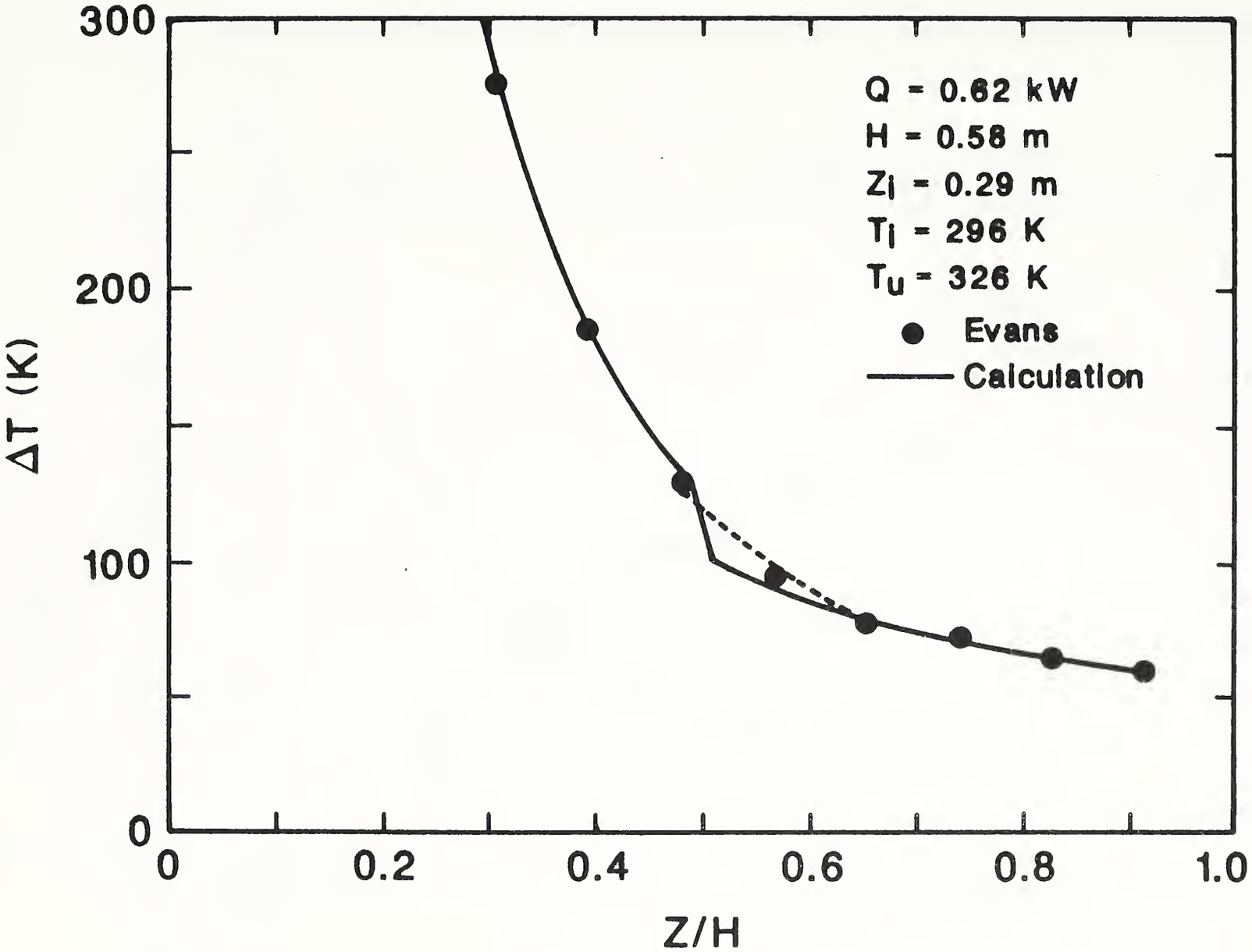

Fig. 1 Comparison of experimental data with prediction in plume centerline temperatures. Solid and dotted lines, calculation; circles, Evans [7].

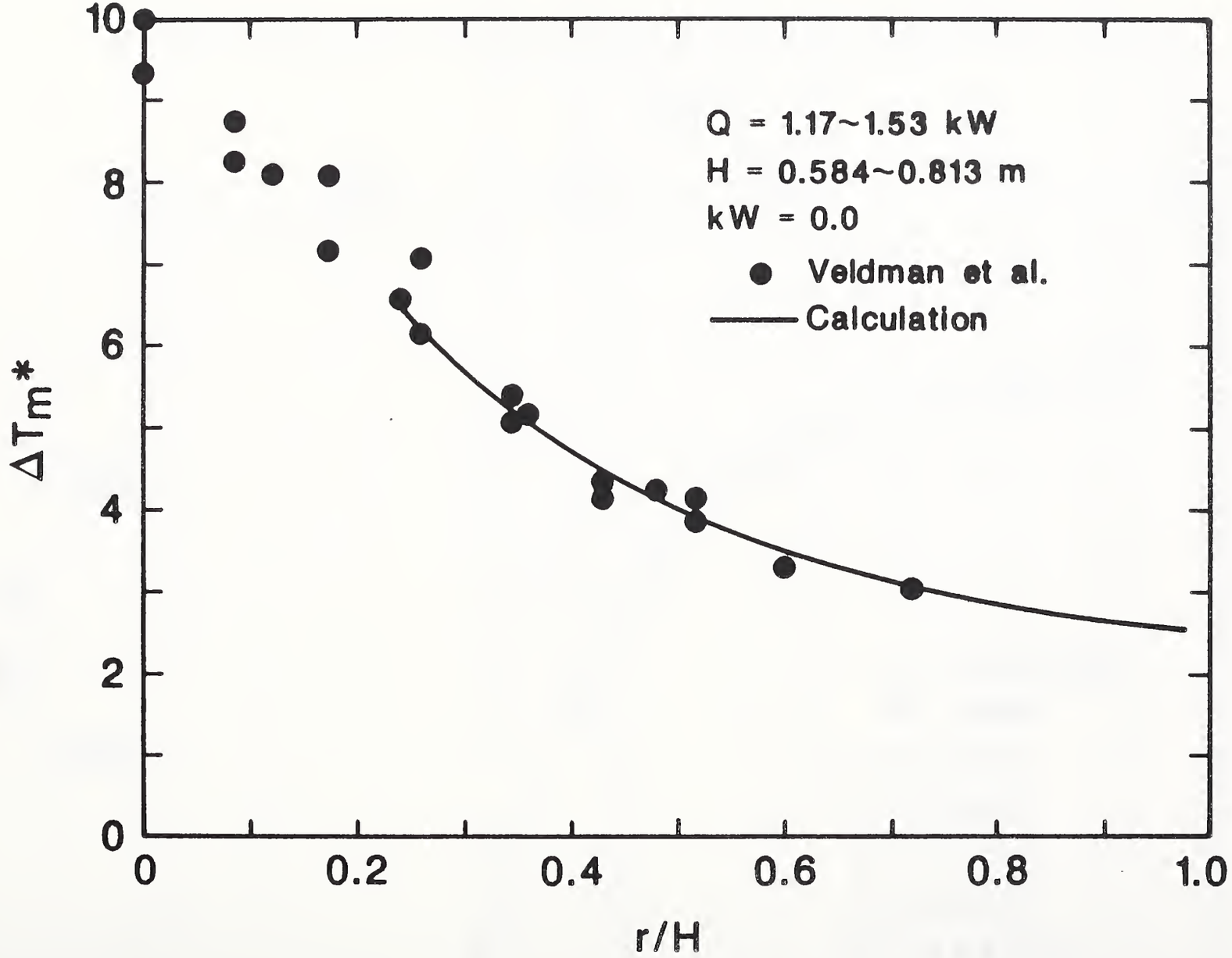

Fig. 2 Comparison of experimental data with prediction in adiabatic (maximum) ceiling-jet temperatures. Solid line, calculation; circles, Veldman et al. [14]. $\Delta T_m^* = \Delta T_m [C^2 \rho^2 g H^5 / (T_\infty Q^2)]^{1/3}$

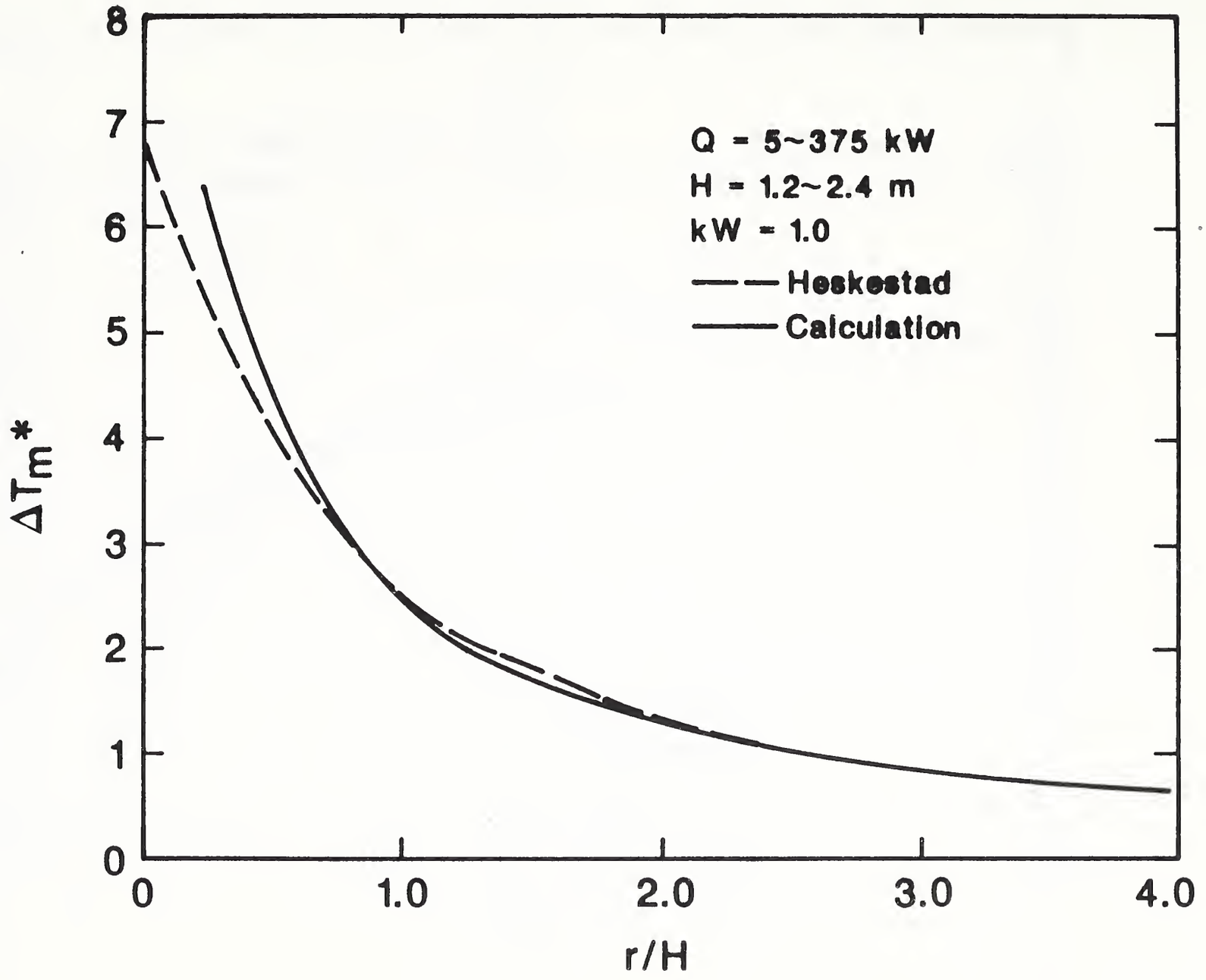

Fig. 3 Comparison between prediction and experimental correlation in maximum excess temperatures of ceiling-jet. Solid line, calculation; dashed line, Heskestad [17]. $\Delta T_m^* = \Delta T_m \, [C_p^2 \rho_a^2 g \, H^5 / (T_a \, Q^2)]^{1/3}$.

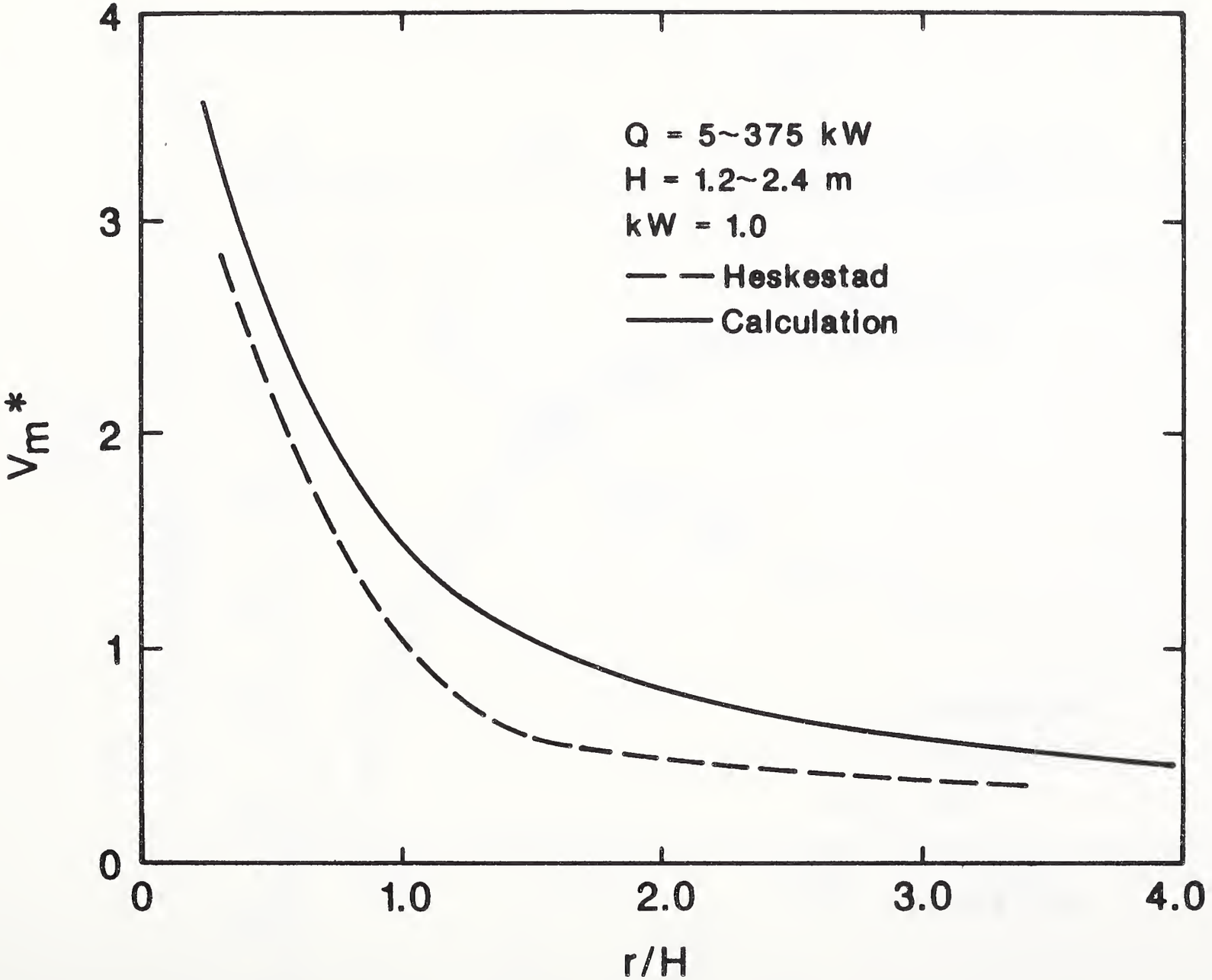

Fig. 4 Comparison between prediction and experimental correlation in radial ceiling-jet velocities. Solid line, calculation; dashed line, Heskestad [17].
$V_m^* = V_m [C_p T_\infty \rho_\infty H / (g Q)]^{1/3}$

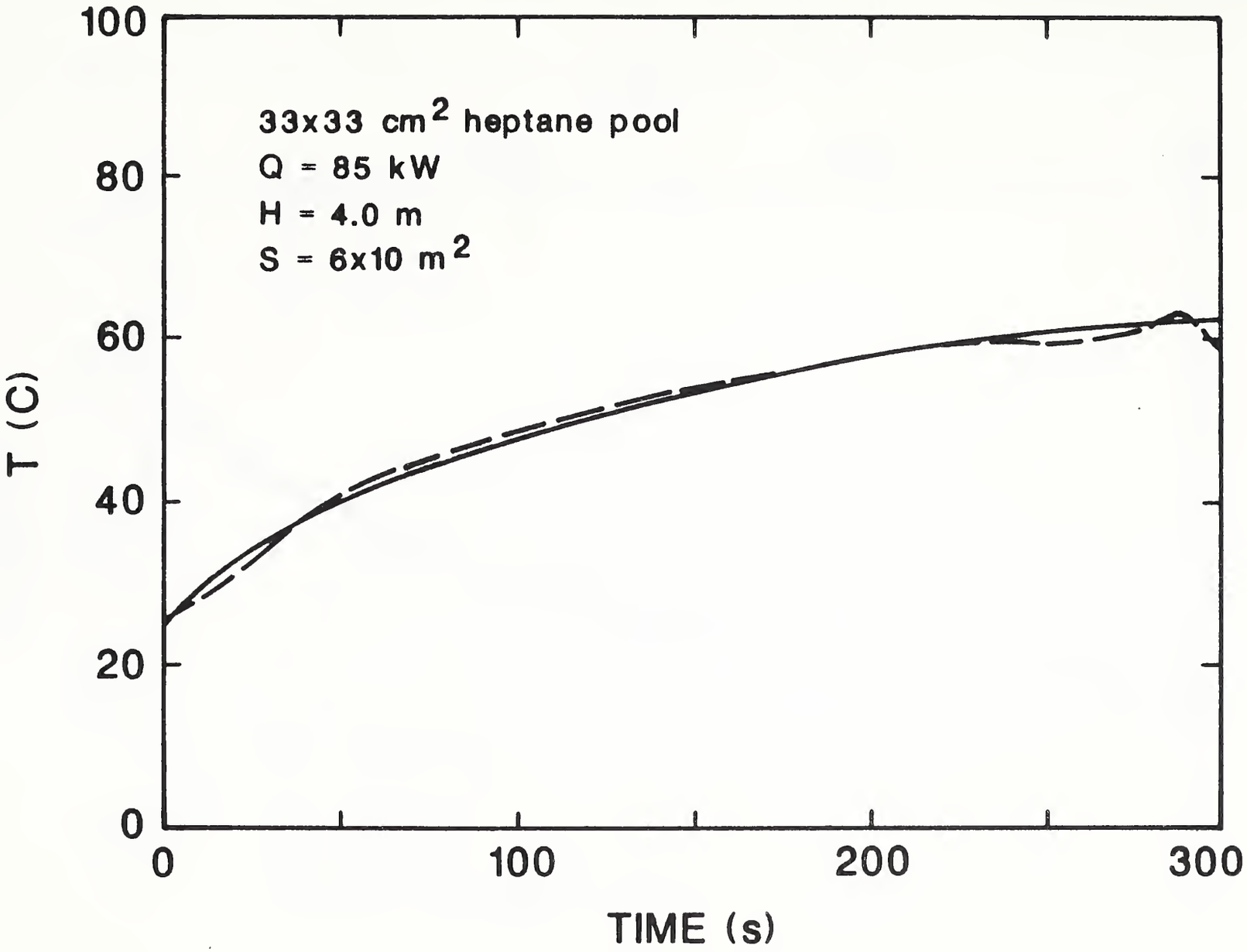

Fig. 5 Comparison of calculated and measured upper-layer temperatures in enclosure. Solid line, calculation; dashed line, experiment. H = 3.0 m.

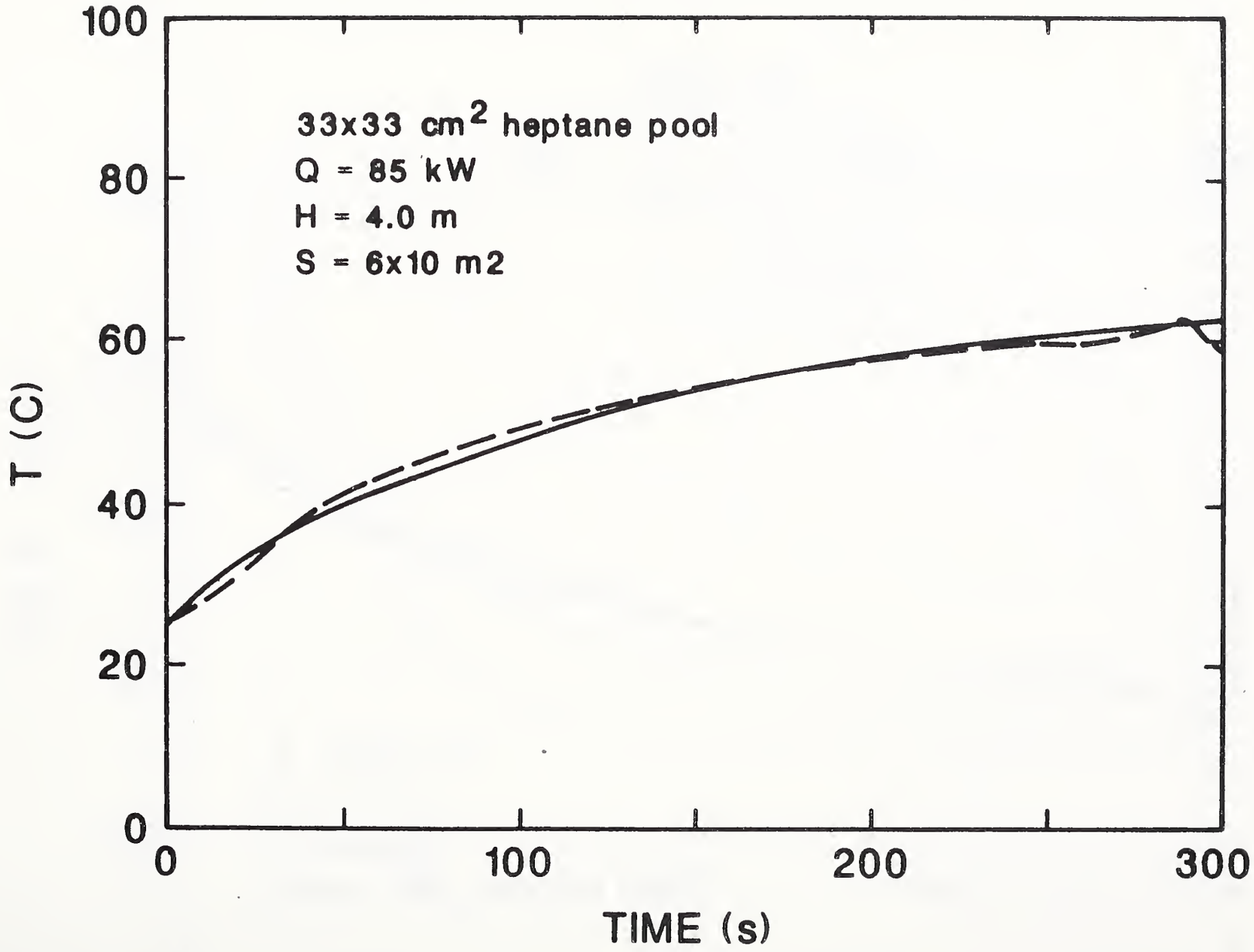

Fig. 6 Comparison of calculated and measured upper-layer temperatures in enclosure. Solid line, calculation; dashed line, experiment. H = 4.0 m.

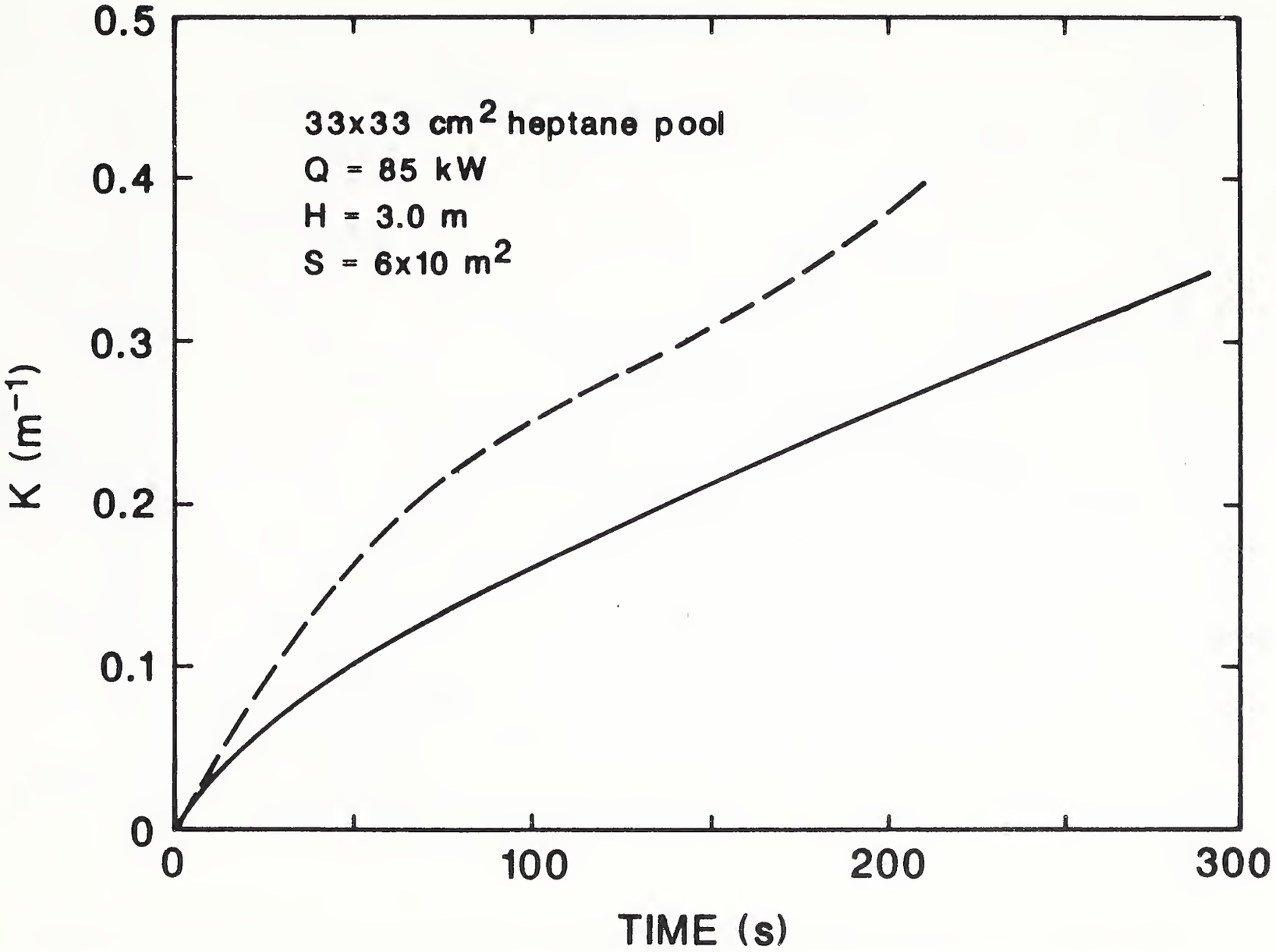

Fig. 7 Comparison of calculated upper-layer smoke concentration with measured ceiling-jet smoke concentration. Solid line, calculation; dashed line, experiment. H = 3.0 m.

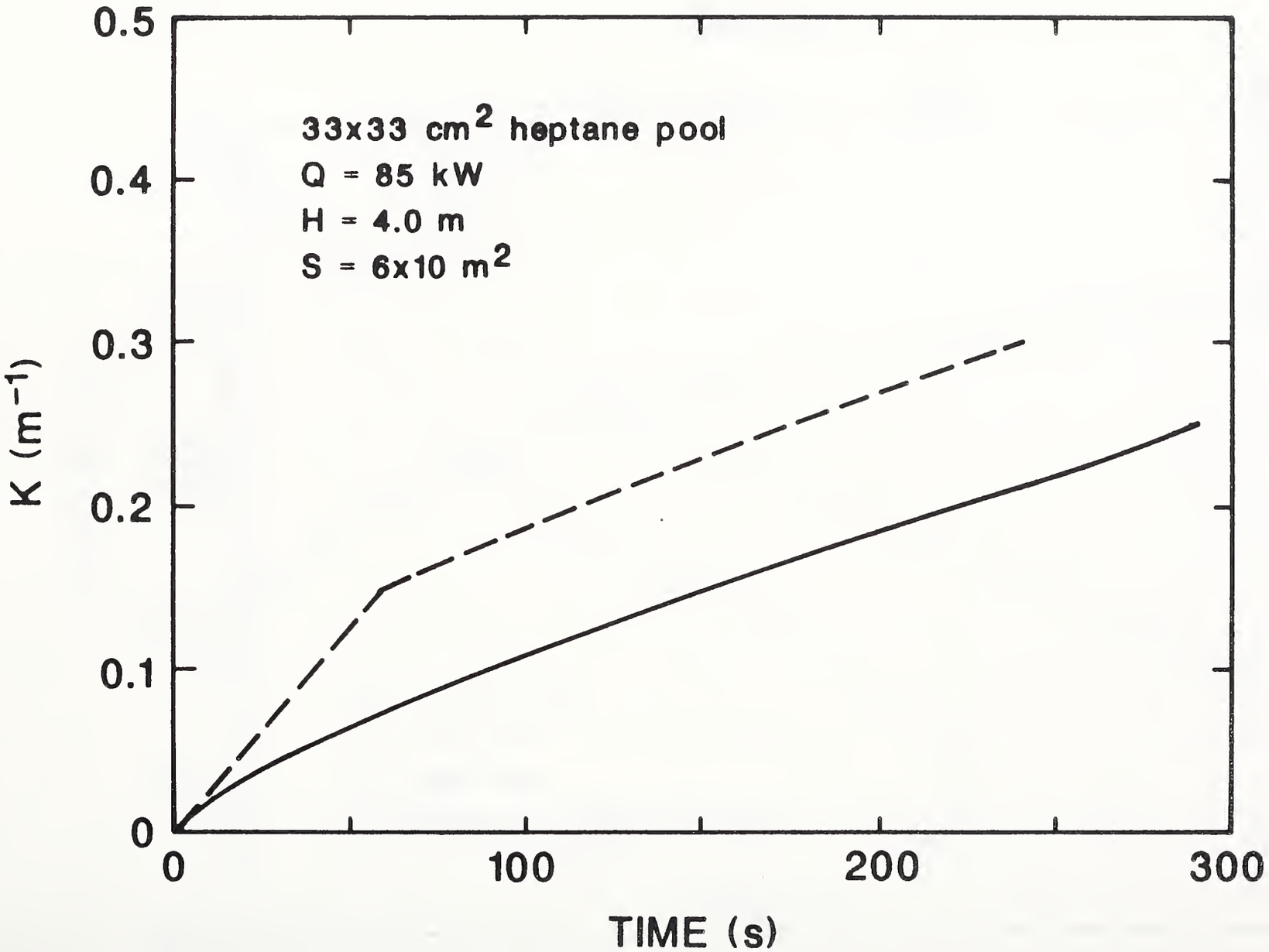

Fig. 8 Comparison of calculated upper-layer smoke concentration with measured ceiling-jet smoke concentration. Solid line, calculation; dashed line, experiment. H = 4.0 m.

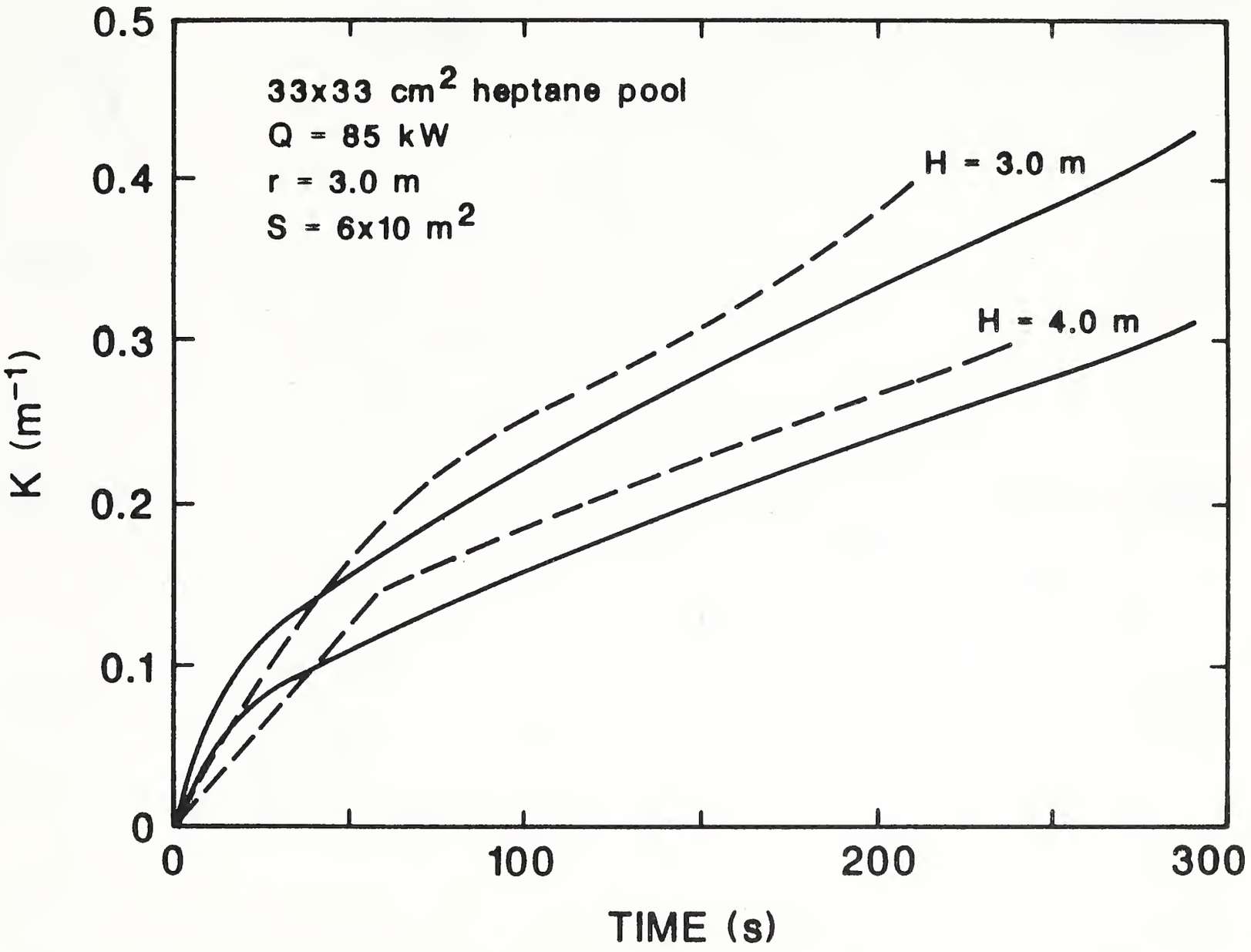

Fig. 9 Comparison between calculated and measured ceiling-jet smoke concentration. Solid lines, calculations; dashed lines, experiments.

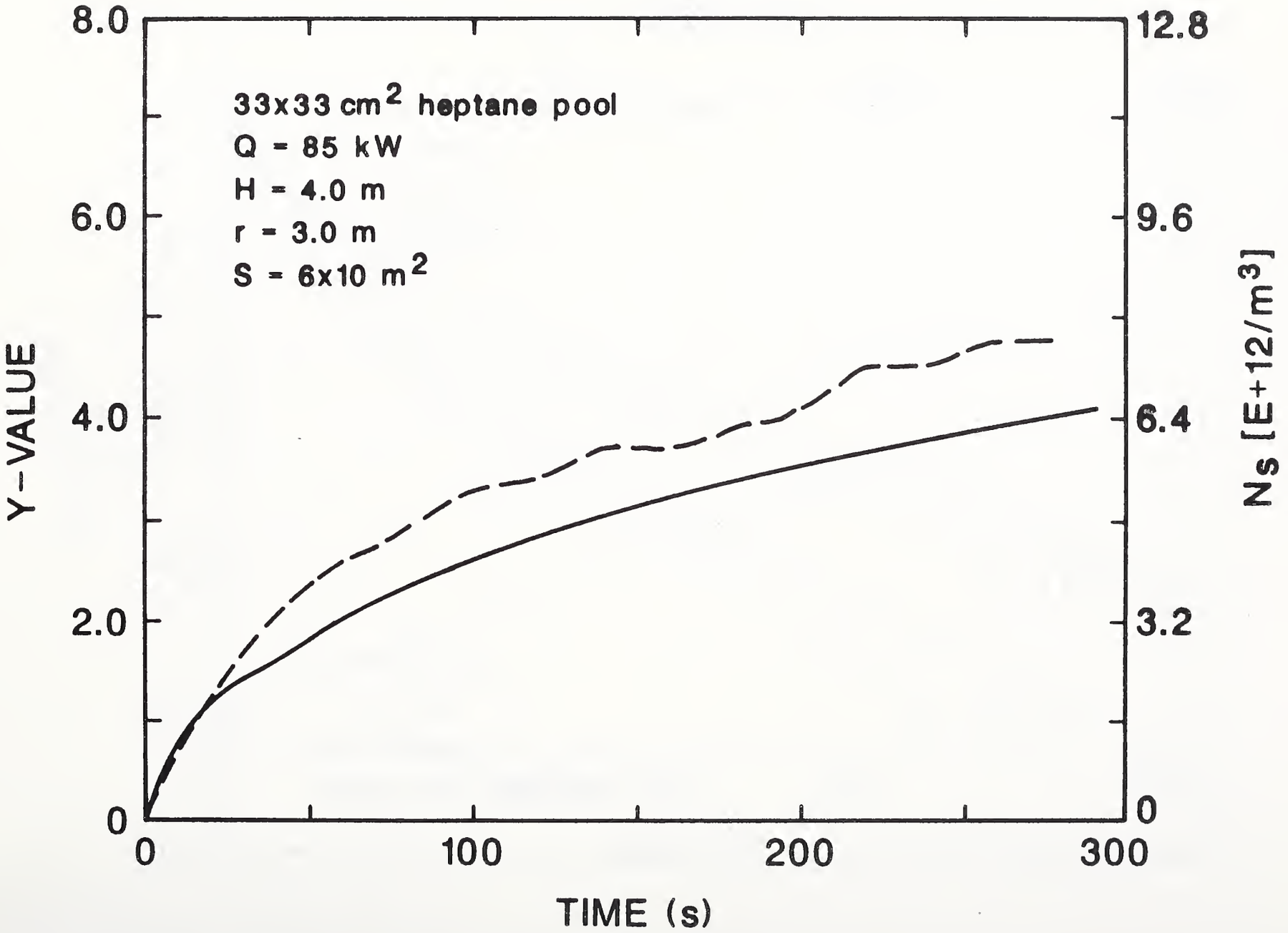

Fig. 10 Comparison between calculated and measured particulate number concentration in ceiling-jet. Solid line, calculation; dashed line,

```
C
      SUBROUTINE SMKINIT
C
      COMMON/SMK/ALFA,BETA,DLTT,EJ0,FW,GCP,GRV,GR0,HCRD,KK,
     . LMD2,MGAS,MGOUT,MSDT,MSTTL,NSDT,NSTTL,PI,PMAS,PR,RCOAG,
     . RDCT,RI0,SP,ST,T0
C
      REAL KK,LMD2,MGAS,MGOUT,MSDT,MSTTL,NSDT,NSTTL
C
      ALFA  = 0.118
      GCP   = 1.007
      GRV   = 9.80665
      GR0   = 1.2046
      LMD2  = 1.157
      T0    = 293.0
C
      BETA  = 3.9
      EJ0   = 0.05
      FW    = 0.025
      KK    = 1.0
      PR    = 0.7030
      RDCT  = 3.0
      SP    = 1.0
      ST    = FW * PR**(-2./3.) / 2.
C
      COAG  = 1.0E-15
      PDIA  = 0.16E-06
      RCOAG = GR0 * COAG
      RSMK  = 2.0E+03
C
      DLTT  = 1.0
      PI    = 3.141592654
      PMAS  = 1./6. * PI * (PDIA**3) * RSMK
C
      MSTTL = 0.0
      NSTTL = 0.0
C
      WRITE(7,700)
C
      RETURN
  700 FORMAT(" TIME ",5X,"TU   ",5X,"DTP  ",5X,"DTJ  ",5X,"CSU  ",5X,
     . "CSP  ",5X,"CSJ  ",5X,"NSU  ",5X,"NSP  ",5X,"NSJ  ",5X,
     . "UP   ",5X,"VJ   ",/)
      END
```

```
C
      SUBROUTINE SMKTPORT
C
C     COMMON BLOCK AND INITIALIZATION FOR THE "FAST" MODEL
C
C
C     NR = MAXIMUM NUMBER OF COMPARTMENTS
C     NN = NUMBER OF NODES IN THE SEPARATORS (WALLS AND CEILINGS)
C     NT = THE MAXIMUM NUMBER OF EQUATIONS TO BE SOLVED (4 * NR)
C     NV = MAXIMUM TIME INTERVALS
C     NS = MAXIMUM NUMBER OF SPECIES TO BE TRACKED
C     NWALL = NUMBER OF DESCRETE WALL SURFACES (CEILING, UPPER WALL ...)
C     MXSLB = MAXIMUM NUMBER OF DIFFERENT MATERIALS IN A WALL
C
      PARAMETER (NR=11, NN = 24, NV = 21, NS = 10)
      PARAMETER (NT = 4*NR+2*NR*NS, MXSLB=3, NWAL=4)
      COMMON/F2C17A/GAMMA,G,SIGM,CP,TA,RA,PREF,RGAS,POFSET,PA,TREF,
     . SS(NR,NR,4),SA(NR,NR,4),AS(NR,NR,4),AA(NR,NR,4),
     . SAU(NR,NR,4),ASL(NR,NR,4),NEUTRAL(6,NR,NR),MINMAS,NLSPCT,
     . QF(2,NR),QR(2,NR),QC(2,NR),QFR(2,NR),QFC(2,NR),
     . EMP(NR),EMS(NR),EME(NR),APS(NR),NWV(NR,NR),RADIUS(NR,NR),IVERS,
     . DDT,LFMAX,QEXP,LFBO,LFPOS,LFBT,QRADRL,HCOMBA,SWITCH(10),
     . BFIRED(NV),AFIRED(NV),HFIRED(NV),TFIRED(NV),TFMAXT,TFIRET,IFIRED,
     . MPRODR(NV,NS), MFIRET(NS),P(NT),PMIN(NT),ZMIN(NR),
     . BW(NR,NR,4),HH(NR,NR,4),HL(NR,NR,4),NW(NR,NR),WINDC(NR),
     . NOPNMX,NRFLOW,HHP(NR,NR,4),HLP(NR,NR,4),WINDV,WINDRF,WINDPW,
     . DELTAT,LPRINT,NSMAX,LDIAGP,LDIAGO,ITMMAX,MAXINR,
     . IST,ITMSTP,IDIAG,DERIV(NT),STIME,NM1,N,N2,N3,N4,
     . BR(NR),DR(NR),HR(NR),AR(NR),HRP(NR),VR(NR),HRL(NR),
     . PW,PM,WC,WH,WO,QP,TE,PPMDV(2,NR,NS),TAMB(NR),RAMB(NR),PAMB(NR),
     . FKW(MXSLB,NWAL,NR),CW(MXSLB,NWAL,NR),RW(MXSLB,NWAL,NR),
     . FLW(MXSLB,NWAL,NR),EPW(NWAL,NR),NDIV(MXSLB,NWAL,NR),NSLB(NWAL,NR)
     . ,TWJ(NWAL,NR,NN),TWE(NWAL,NR),QSRADW(2,NR),QSCNV(2,NR),HFLR(NR),
     . MASS(2,NR,NS), TOXICT(2,NR,NS), PPM(2,NR,NS), ACTIVS(NS),
     . NCONFG,NDUMPR,LCOPY,CFILE,DFILE,TITLE,TERMXX
      CHARACTER CFILE(5)*17, TITLE(50)*1, DFILE*17
      REAL MASS,MPRODR,MFIRET,MINMAS,LC50CF,NEUTRAL
      LOGICAL ACTIVS,SWITCH
C
      COMMON/SMK/ALFA,BETA,DLTT,EJ0,FW,GCP,GRV,GR0,HCRD,KK,
     . LMD2,MGAS,MGOUT,MSDT,MSTTL,NSDT,NSTTL,PI,PMAS,PR,RCOAG,
     . RDCT,RI0,SP,ST,T0
C
      REAL KK,LMD2,MGAS,MGOUT,MSDT,MSTTL,NSDT,NSTTL
C
      DIMENSION WRK(2)
      EXTERNAL FSMK
C
      OLDMAS = RAMB(1) * TAMB(1) / P(N+1) * P(N2+1)
C
      MGAS   = MAX(OLDMAS,MINMAS)
      MGOUT  = SS(1,2,1) + SA(1,2,1)
      MSDT   = MFIRET(9)
      NSDT   = MFIRET(9) / PMAS
```

```
C
      WRK(1) = MSTTL
      WRK(2) = NSTTL
C
      CALL RKCAL (FSMK, TIME, DLTT, 2, WRK)
C
      MSTTL  = WRK(1)
      NSTTL  = WRK(2)
C
      RETURN
      END
C
```

```
      SUBROUTINE FSMK (F, X, Y)
C
      DIMENSION F(2),Y(2)
C
      COMMON/SMK/ALFA,BETA,DLTT,EJ0,FW,GCP,GRV,GR0,HCRD,KK,
     . LMD2,MGAS,MGOUT,MSDT,MSTTL,NSDT,NSTTL,PI,PMAS,PR,RCOAG,
     . RDCT,RI0,SP,ST,T0
C
      REAL KK,LMD2,MGAS,MGOUT,MSDT,MSTTL,NSDT,NSTTL
C
      F(1) = MSDT - Y(1)*(MGOUT/MGAS)
      F(2) = NSDT - RCOAG/MGAS*(Y(2)**2) - Y(2)*(MGOUT/MGAS)
C
      RETURN
      END
C
```

```
      SUBROUTINE SMKRESLT (TIME)
C
C     COMMON BLOCK AND INITIALIZATION FOR THE "FAST" MODEL
C
C
C     NR = MAXIMUM NUMBER OF COMPARTMENTS
C     NN = NUMBER OF NODES IN THE SEPARATORS (WALLS AND CEILINGS)
C     NT.= THE MAXIMUM NUMBER OF EQUATIONS TO BE SOLVED (4 * NR)
C     NV = MAXIMUM TIME INTERVALS
C     NS = MAXIMUM NUMBER OF SPECIES TO BE TRACKED
C     NWALL = NUMBER OF DESCRETE WALL SURFACES (CEILING, UPPER WALL ...)
C     MXSLB = MAXIMUM NUMBER OF DIFFERENT MATERIALS IN A WALL
C
      PARAMETER (NR=11, NN = 24, NV = 21, NS = 10)
      PARAMETER (NT = 4*NR+2*NR*NS, MXSLB=3, NWAL=4)
      COMMON/F2C17A/GAMMA,G,SIGM,CP,TA,RA,PREF,RGAS,POFSET,PA,TREF,
     . SS(NR,NR,4),SA(NR,NR,4),AS(NR,NR,4),AA(NR,NR,4),
     . SAU(NR,NR,4),ASL(NR,NR,4),NEUTRAL(6,NR,NR),MINMAS,NLSPCT,
     . QF(2,NR),QR(2,NR),QC(2,NR),QFR(2,NR),QFC(2,NR),
     . EMP(NR),EMS(NR),EME(NR),APS(NR),NWV(NR,NR),RADIUS(NR,NR),IVERS,
     . DDT,LFMAX,QEXP,LFBO,LFPOS,LFBT,QRADRL,HCOMBA,SWITCH(10),
     . BFIRED(NV),AFIRED(NV),HFIRED(NV),TFIRED(NV),TFMAXT,TFIRET,IFIRED,
     . MPRODR(NV,NS), MFIRET(NS),P(NT),PMIN(NT),ZMIN(NR),
     . BW(NR,NR,4),HH(NR,NR,4),HL(NR,NR,4),NW(NR,NR),WINDC(NR),
     . NOPNMX,NRFLOW,HHP(NR,NR,4),HLP(NR,NR,4),WINDV,WINDRF,WINDPW,
     . DELTAT,LPRINT,NSMAX,LDIAGP,LDIAGO,ITMMAX,MAXINR,
     . IST,ITMSTP,IDIAG,DERIV(NT),STIME,NM1,N,N2,N3,N4,
     . BR(NR),DR(NR),HR(NR),AR(NR),HRP(NR),VR(NR),HRL(NR),
     . PW,PM,WC,WH,WO,QP,TE,PPMDV(2,NR,NS),TAMB(NR),RAMB(NR),PAMB(NR),
     . FKW(MXSLB,NWAL,NR),CW(MXSLB,NWAL,NR),RW(MXSLB,NWAL,NR),
     . FLW(MXSLB,NWAL,NR),EPW(NWAL,NR),NDIV(MXSLB,NWAL,NR),NSLB(NWAL,NR)
     . ,TWJ(NWAL,NR,NN),TWE(NWAL,NR),QSRADW(2,NR),QSCNV(2,NR),HFLR(NR),
     . MASS(2,NR,NS), TOXICT(2,NR,NS), PPM(2,NR,NS), ACTIVS(NS),
     . NCONFG,NDUMPR,LCOPY,CFILE,DFILE,TITLE,TERMXX
      CHARACTER CFILE(5)*17, TITLE(50)*1, DFILE*17
      REAL MASS,MPRODR,MFIRET,MINMAS,LC50CF,NEUTRAL
      LOGICAL ACTIVS,SWITCH
C
      COMMON/SMK/ALFA,BETA,DLTT,EJ0,FW,GCP,GRV,GR0,HCRD,KK,
     . LMD2,MGAS,MGOUT,MSDT,MSTTL,NSDT,NSTTL,PI,PMAS,PR,RCOAG,
     . RDCT,RI0,SP,ST,T0
      COMMON/HFOT/HFOT
C
      REAL KK,LMD2,MGAS,MGOUT,MSDT,MSTTL,NSDT,NSTTL
      REAL NSJ,NSP,NSU
C
      BP   = 0.0
      CSP  = 0.0
      DTP  = 0.0
      NSP  = 0.0
      UP   = 0.0
C
      CSJ  = 0.0
      DTJ  = 0.0
```

```
      HJ   = 0.0
      NSJ  = 0.0
      VJ   = 0.0
C
      CSU  = MSTTL / P(N2+1)
      NSU  = NSTTL / P(N2+1)
C
      TL   = P(N3+1)
      TU   = P(N+1)
      TDF  = TU - TL
      TW   = TWJ(1,1,1)
      QPLM = QFC(1,1) + (-QP+CP*(TE-TL))*EMP(1)
      ZJ0  = (HR(1) - HFOT) / (1. + (6.**.5 /5.) * ALFA)
      ZU   = P(N2+1) / AR(1)
      ZD   = (HCRD - (HRP(1) - ZU)) * 0.5
      ZI   = HR(1) - HFOT - ZU
C
      IF (QPLM .LT. 0.01) THEN
         CSP = CSU
         DTP = TDF
         NSP = NSU
         GO TO 100
      ENDIF
      CALL PLUME2 (CSU,QPLM,MSDT,NSDT,NSU,TDF,TL,ZI,ZJ0,
     . BP,CSP,DTP,NSP,UP)
  100 CONTINUE
C
      IF (UP .LT. 0.01) THEN
         CSJ = CSU
         DTJ = TDF
         NSJ = NSU
         GO TO 200
      ENDIF
      CALL CLGJET (BP,CSP,CSU,DTP,NSU,NSP,RDCT,TDF,TL,TW,UP,
     . CSJ,DTJ,NSJ,HJ,VJ)
  200 CONTINUE
C
      WRITE(7,700) TIME,TU,DTP,DTJ,CSU,CSP,CSJ,NSU,NSP,NSJ,UP,VJ
C
      RETURN
  700 FORMAT(1P12E10.3)
      END
C
```

```
      SUBROUTINE PLUME2 (CSU,Q,QS,QN,NSU,TDF,TL,ZI,ZJ0,
     . BB,CSM,DTM,NSM,UM)
C
      COMMON/SMK/ALFA,BETA,DLTT,EJ0,FW,GCP,GRV,GR0,HCRD,KK,
     . LMD2,MGAS,MGOUT,MSDT,MSTTL,NSDT,NSTTL,PI,PMAS,PR,RCOAG,
     . RDCT,RI0,SP,ST,T0
C
      REAL KK,LMD2,MGAS,MGOUT,MSDT,MSTTL,NSDT,NSTTL
      REAL NSM,NSU
C
      DIMENSION WRK(3)
      EXTERNAL FPLM
C
      DZ  = 0.1
      TU  = TL + TDF
      ZF  = 0.08 * Q**(2./5.)
C
      F1  = Q*GRV*(LMD2+1.) / (PI*GR0*GCP*T0)
      FS1 = QS*(LMD2+1.) / PI
      FN1 = QN*(LMD2+1.) / PI
C
      IF (ZI .LT. ZF) GO TO 200
C
      Z   = ZI
      IF (ZI .GT. ZJ0) Z = ZJ0
C
      V   = (9./5.*F1*ALFA)**(1./3.) * Z**(2./3.)
      W   = 6./5. * ALFA * (9./5.*F1*ALFA)**(1./3.) * Z**(5./3.)
      BB  = W / V
      UM  = (V*V) / W
      DTM = F1/(LMD2*GRV*W) * TL
      CSM = FS1 / (LMD2*W)
      NSM = FN1 / (LMD2*W)
      IF (Z .GT. ZJ0-DZ/2.) RETURN
C
      F2  = LMD2*GRV*W * (DTM - (LMD2+1.)/LMD2 * TDF) / TL
      FS2 = LMD2*W * (CSM - (LMD2+1.)/LMD2 * CSU)
      FN2 = LMD2*W * (NSM - (LMD2+1.)/LMD2 * NSU)
C
      IF (F2 .LT. 1.0E-04) THEN
         BB  = 0.0
         CSM = CSU
         DTM = TU
         NSM = NSU
         UM  = 0.0
         RETURN
      ENDIF
C
      WRK(1) = W
      WRK(2) = V
      WRK(3) = F2
C
  100 CALL RKCAL(FPLM,Z,DZ,3,WRK)
C
```

```
      Z  = Z + DZ
      IF (Z .LE. ZJ0-DZ/2.) GO TO 100
C
      W  = WRK(1)
      V  = WRK(2)
      GO TO 300
C
  200 F2   = F1
      FS2  = FS1
      FN2  = FN1
      DLTZ = ((F1/F2)**.5 - 1.) * ZI
      Z2   = ZJ0 + DLTZ
      V    = (9./5.*F2*ALFA)**(1./3.) * Z2**(2./3.)
      W    = 6./5. * ALFA * (9./5.*F2*ALFA)**(1./3.) * Z2**(5./3.)
  300 BB   = W / V
      UM   = (V*V) / W
      DTM  = MAX(F2/(LMD2*GRV*W)*TU+TDF, F1/(LMD2*GRV*W)*TL)
      CSM  = MAX(FS2/(LMD2*W)+CSU, FS1/(LMD2*W))
      NSM  = MAX(FN2/(LMD2*W)+NSU, FN1/(LMD2*W))
C
      RETURN
      END
C
```

```
      SUBROUTINE FPLM (F, X, Y)
C
      COMMON/SMK/ALFA,BETA,DLTT,EJ0,FW,GCP,GRV,GR0,HCRD,KK,
     . LMD2,MGAS,MGOUT,MSDT,MSTTL,NSDT,NSTTL,PI,PMAS,PR,RCOAG,
     . RDCT,RI0,SP,ST,T0
C
      DIMENSION F(3),Y(3)
C
      F(1) = 2. * ALFA * Y(2)
      F(2) = Y(3) * Y(1) / Y(2)**3
      F(3) = 0.0
C
      RETURN
      END
C
```

```
      SUBROUTINE CLGJET (BB,CSP,CSU,DTP,NSU,NSP,RMX,TDF,TL,TW,UM,
     . CSJ,DTJ,NSJ,HH,VM)
C
      COMMON/SMK/ALFA,BETA,DLTT,EJ0,FW,GCP,GRV,GR0,HCRD,KK,
     . LMD2,MGAS,MGOUT,MSDT,MSTTL,NSDT,NSTTL,PI,PMAS,PR,RCOAG,
     . RDCT,RI0,SP,ST,T0
C
      REAL KK,LMD2,MGAS,MGOUT,MSDT,MSTTL,NSDT,NSTTL
      REAL NSA,NSA0,NSJ,NSP,NSU
C
      DIMENSION WRK(3)
      EXTERNAL FJET
C
      DR   = 0.1
      TA   = TL + TDF
      CSA0 = LMD2 / (LMD2+1.) * (CSP - CSU)
      DTA0 = LMD2 / (LMD2+1.) * (DTP - TDF)
      HA0  = BB / 6.**.5
      NSA0 = LMD2 / (LMD2+1.) * (NSP - NSU)
      VA0  = UM / 2.**.5
      RI0  = GRV*(DTA0/TA)*HA0 / (VA0*VA0)
      R0   = 3.**.5 * BB
C
      CSA  = CSA0
      DTA  = DTA0
      HA   = HA0
      NSA  = NSA0
      R    = R0
      RI   = RI0
      SGM  = 0.0
      VA   = VA0
C
      IF (R0 .GT. RMX-DR/2.) GO TO 200
C
      WRK(1) = HA0
      WRK(2) = RI0
      WRK(3) = 0.0
C
  100 CALL RKCAL (FJET,R,DR,3,WRK)
      R  = R + DR
      IF (R .LE. RMX-DR/2.) GO TO 100
C
      HA   = WRK(1)
      RI   = WRK(2)
      SGM  = WRK(3)
C
  200 DMY  = EXP(-KK*ST/3.*SGM)
      VA   = VA0 * (RI/RI0 * R/R0)**(-1./3.) * DMY
      CSA  = CSA0 * R0*HA0*VA0 / (R*HA*VA)
      DTA  = DTA0 * HA0/HA * (R0/R*R0/R*RI/RI0)**(1./3.) * DMY*DMY
      NSA  = NSA0 * R0*HA0*VA0 / (R*HA*VA)
C
      CSJ  = CSA * ((LMD2+1.)/LMD2)**.5 + CSU
      DTJ  = DTA * ((LMD2+1.)/LMD2)**.5 + TDF
```

```
      NSJ   = NSA * ((LMD2+1.)/LMD2)**.5 + NSU
      HH    = HA  / (PI/2.)**.5
      VM    = VA  * 2.**.5
C
      RETURN
      END
C
```

```
      SUBROUTINE FJET (F, X, Y)
C
      COMMON/SMK/ALFA,BETA,DLTT,EJ0,FW,GCP,GRV,GR0,HCRD,KK,
     . LMD2,MGAS,MGOUT,MSDT,MSTTL,NSDT,NSTTL,PI,PMAS,PR,RCOAG,
     . RDCT,RI0,SP,ST,T0
C
      REAL KK,LMD2,MGAS,MGOUT,MSDT,MSTTL,NSDT,NSTTL
C
      DIMENSION F(3),Y(3)
C
      EJ = EJ0 * EXP(BETA*(RI0-Y(2)))
C
      F(1) = (FW/2. + (2.- SP*Y(2)/2.)*EJ - Y(1)/X - SP*Y(2)*KK*ST/2.)
     .     / (1. - SP*Y(2))
      F(2) = (FW/2. + (1.+ SP*Y(2)/2.) * (EJ - KK*ST/3.)
     .     - (1.+ 2.*SP*Y(2)) * Y(1)/(3.*X))
     .     / ((1.- SP*Y(2)) * Y(1)/(3.*Y(2)))
      F(3) = 1./ Y(1)
C
      RETURN
      END
C
```

FORM NBS-114A (REV.11-84)

U.S. DEPT. OF COMM. **BIBLIOGRAPHIC DATA SHEET** *(See instructions)*	1. PUBLICATION OR REPORT NO. NBSIR-88-3707	2. Performing Organ. Report No.	3. Publication Date January 1988

4. TITLE AND SUBTITLE

Prediction of Response Time of Smoke Detectors in Enclosure Fires

5. AUTHOR(S) Yukio Yamauchi

6. PERFORMING ORGANIZATION *(If joint or other than NBS, see instructions)*

NATIONAL BUREAU OF STANDARDS
U.S. DEPARTMENT OF COMMERCE
GAITHERSBURG, MD 20899

7. Contract/Grant No.

8. Type of Report & Period Covered

Final

9. SPONSORING ORGANIZATION NAME AND COMPLETE ADDRESS *(Street, City, State, ZIP)*

Hochiki Corporation
246 Tsuruma, Machida-shi
Tokyo 194 JAPAN

10. SUPPLEMENTARY NOTES

☐ Document describes a computer program; SF-185, FIPS Software Summary, is attached.

11. ABSTRACT *(A 200-word or less factual summary of most significant information. If document includes a significant bibliography or literature survey, mention it here)*

In order to predict the response time of smoke detectors in enclosure fires, a computational model is developed for calculating the local particulate concentration near the ceiling. The large scale smoke movement is approximated by integral equations for plume and ceiling-jet, which originates in the cold lower layer and penetrates into the accumulated smoke layer in the upper portion of enclosure. The effect of coagulation, which changes the particle size distribution, is included to enable predictions of ionization smoke detector response. This engineering model is designed to be used in combination with two-layer zone models for obtaining more detailed information of smoke concentration in the upper layer. Sample calculations have been made and comparisons with relevant experimental data showed a reasonable agreement both in the mass concentration and particle number concentration of smoke in the ceiling-jet.

12. KEY WORDS *(Six to twelve entries; alphabetical order; capitalize only proper names; and separate key words by semicolons)*

computer programs; fire models; ionization detectors; particle density (concentration); photoelectric detectors; response time; zone models

13. AVAILABILITY

☒ Unlimited

☐ For Official Distribution. Do Not Release to NTIS

☐ Order From Superintendent of Documents, U.S. Government Printing Office, Washington, DC 20402.

☒ Order From National Technical Information Service (NTIS), Springfield, VA 22161

14. NO. OF PRINTED PAGES 52

15. Price $13.95